NATIONAL ENERGY TECHNOLOGY LABORATORY

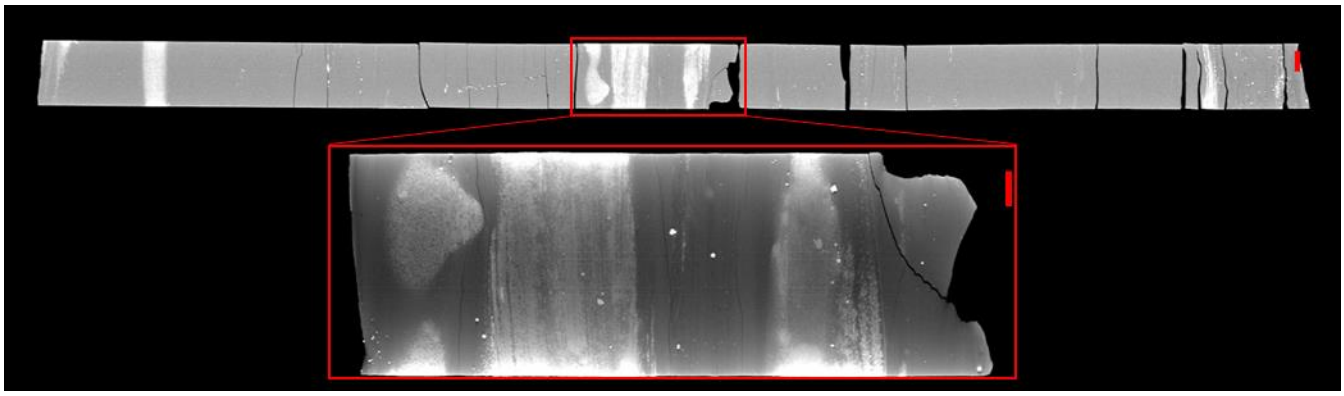

Computed Tomography Scanning and Petrophysical Measurements of Illinois Basin Coal Wells

22 January 2024

U.S. DEPARTMENT OF ENERGY | NATIONAL ENERGY TECHNOLOGY LABORATORY

Office of Fossil Energy and Carbon Management

DOE/NETL-2024/4799

Disclaimer

This project was funded by the United States Department of Energy, National Energy Technology Laboratory, in part, through a site support contract.

Cover Illustration: Medical computed tomography (CT) image of the Weatherford Well from 262 to 266 ft; and an industrial CT image at 264 ft at 36.8 μm^3 voxel resolution.

Suggested Citation: Paronish, T.; Crandall, D.; Jarvis, K.; Workman, S.; Drosche, J.; Pohl, M.; Mckisic, T.; McLaughlin P.; Friedberg, J.; Delpomdor F. *Computed Tomography Scanning and Petrophysical Measurements of Illinois Basin Coal Wells;* DOE/NETL-2024/4799; NETL Technical Report Series; U.S. Department of Energy, National Energy Technology Laboratory: Morgantown, WV, 2024; p 56. https://doi.org/10.2172/2282147

An electronic version of this report can be found at:

https://edx.netl.doe.gov/group/core-characterization

https://netl.doe.gov/energy-analysis/search

The data in this report can be accessed from NETL's Energy Data eXchange (EDX) online system (https://edx.netl.doe.gov) using the following link:

https://edx.netl.doe.gov/dataset/illinois-basin-coal-wells

Computed Tomography Scanning and Petrophysical Measurements of Illinois Basin Coal Wells

Thomas Paronish[1,2]; Dustin Crandall[1]; Karl Jarvis[1,2]; Scott Workman[1,2]; Jessica Drosche[1,2]; Mathias Pohl[1,2]; Terry Mckisic[1,2]; Jared Friedburg[3]; Pat McLaughlin[3]; Franck Delpomdor[3]

[1]National Energy Technology Laboratory, 3610 Collins Ferry Road, Morgantown, WV 26505, USA

[2]NETL Support Contractor, 3610 Collins Ferry Road, Morgantown, WV 26505, USA

[3]Illinois State Geological Survey, 615 E Peabody Drive, Champaign, IL 61820, USA

DOE/NETL-2024/4799

22 January 2024

NETL Contacts:

Dustin Crandall, Principal Investigator

R. Burt Thomas, Technical Portfolio Lead

Bryan Morreale, Associate Laboratory Director for Research & Innovation, Research & Innovation Center

This page intentionally left blank.

Table of Contents

List of Figures

List of Figures (cont.)

List of Tables

Acronyms, Abbreviations, and Symbols

Term	Description
2D	Two-dimensional
3D	Three-dimensional
CT	Computed tomography
CTN	CT number
d	Sample thickness
DOE	U.S. Department of Energy
EDX	NETL's Energy Data eXchange
HU	Hounsfield Unit
H	External magnetic field
I	Measured Intensity
ISGS	Illinois State Geological Survey
I_0	Source Intensity
J	Magnetic response (per unit volume)
k	Volume susceptibility
MSCL	Multi-Sensor Core Logger
NETL	National Energy Technology Laboratory
REE	Rare earth elements
XRF	X-ray fluorescence
μ	Compton attenuation coefficient
ρ	Bulk Density

Acknowledgments

This work was completed at the National Energy Technology Laboratory (NETL) with support from the U.S. Department of Energy's (DOE) Office of Fossil Energy Oil & Gas Program. The authors wish to acknowledge Bryan Morreale (NETL Research & Innovation Center), Jessica Mullins and Scott Montross (NETL Science & Technology Strategic Plans and Programs), and Anna Wendt (DOE Office of Fossil Energy and Carbon Management) for programmatic guidance, direction, and support.

The authors would like to thank Bryan Tennant for computed tomography data collection and technical support. Thank you to the staff of the Geologic Characterization, Analytics, and Modeling laboratory at NETL for continued laboratory support.

ABSTRACT

The computed tomography (CT) facilities and the Multi-Sensor Core Logger (MSCL) at the U.S. Department of Energy's (DOE) National Energy Technology Laboratory (NETL) in Morgantown, West Virginia, were used to characterize core from four wells that represent coal resources across Illinois. These include the:

- Brush Creek Quarry Well (API: 12-173-2432400) in Shelby County, IL
- E. Miller/Hanna City Well (API: 12-143-3548100) in Peoria County, IL
- Morris Well (API: 12-199-2399600) in Williamson County, IL
- Weatherford Well (API: 12-145-2892900) in Perry County, IL

The primary impetus of this work was to capture a detailed digital representation of the core from the Brush Creek Quarry, E. Miller/Hanna City, Morris, and Weatherford Wells. The collaboration between the NETL and the Illinois State Geological Survey (ISGS) enables other research entities to access information about this potential carbon ore, rare earth, and critical mineral resource play in the Illinois Basin. The resultant datasets are presented in this report and can be accessed from NETL's Energy Data eXchange (EDX) online system using the following link: https://edx.netl.doe.gov/dataset/illinois-basin-coal-wells.

All equipment and techniques used were non-destructive, enabling future examinations and analyses to be performed on these cores. Fractures, discontinuities, and millimeter-scale features were readily detectable with the medical CT scanner acquired images. Imaging with the NETL medical CT scanner was performed on entire cores. Qualitative analysis of the medical CT images, coupled with X-ray fluorescence (XRF), gamma density, and magnetic susceptibility measurements from the MSCL were useful in identifying zones of interest for potential future analysis. Higher-resolution industrial and micro-CT images were acquired from selected zones along the depth of the core to visualize the structure in higher detail. The ability to quickly identify key areas for more detailed study with higher resolution will save time and resources in future studies. The combination of methods used provides a multi-scale analysis of the core, with the resulting macro- and micro-descriptions relevant to many subsurface energy related examinations traditionally performed at NETL.

1. INTRODUCTION

Evaluation of coal basin strata for identification of critical minerals and rare earth elements is an essential part of fulfilling the nation's goal of sustainable energy transition from fossil energy and builds a more robust accounting of national reserves. As part of this effort, this technical report provides non-destructive characterization of a potential resource utilizing computed tomography (CT) imaging and petrophysical measurements via the multi-sensor core logger (MSCL) at the U.S. Department of Energy's (DOE) National Energy Technology Laboratory (NETL). While it is common for commercial entities to perform these characterizations, the resources necessary to conduct these analyses are not always available to the broader interest base, such as state agencies and research-based consortia. To meet the growing need for comprehensive and high-quality lithologic data for collaborative research initiatives, NETL uses available resources to develop a systematic approach for the evaluation of subsurface geological core materials.

The data is presented in several formats here and online at NETL's Energy Data eXchange (EDX) (https://edx.netl.doe.gov/dataset/illinois-basin-coal-wells). These data are potentially useful for various analyses. However, little detailed analysis is presented in this report as the research objective was not to perform site characterizations, but rather to acquire the data for others to utilize and to create a digital representation of the core that could be preserved in perpetuity.

1.1 SITE BACKGROUND

Sections of four wells from across the Illinois Basin were characterized:

- Brush Creek Quarry Well (API: 12-173-24324-00) drilled in Shelby County, IL (Figure 1, dark orange star)
- E. Miller/Hanna City Well (API: 12-143-35481-00) drilled in Peoria County, IL (Figure 1, dark yellow star)
- Morris Well (API: 12-199-23996-00) drilled in Williamson County, IL (Figure 1, light orange star).
- Weatherford Well (API: 12-145-28929-00) drilled in Perry County, IL (Figure 1, light yellow star)

The wells were drilled for exploration of coal resources in the Mattoon, Shelburn, Carbondale, and Tradewater formations. Full details are available in Table 1.

Figure 1: Location map of wells in this report; dark orange star - Brush Creek Quarry Well, dark yellow star - E. Miller/Hanna City Well, light orange star - Morris Well, and light-yellow star - Weatherford Well.

Table 1: Detailed List of Core Intervals, Well Colors are Related to the Star Colors in Figure 1

Number	Latitude (NAD83DD)	Longitude (NAD83DD)	API	County	State	Boxes	Depth (ft)	Formation	Coal unit
Brush Creek Quarry	39.285	-88.708	121732432400	Shelby	IL	22 - 23	202 - 221	Mattoon	Opdyke
						25 - 27	231 - 261	Mattoon	Cohn
E. Miller/ Hanna City	40.915	-89.611	121433548100	Peoria	IL	11 - 13	103 - 132	Shelburn	Danville
						15 - 16	141.5 - 160.1	Carbondale	Herrin
						22 - 25	207.2 - 243.9		Springfield
						26 - 27	243.9 - 262.5		Houchin Creek
						33 - 35	310.6 - 339.1		Colchester
Morris	37.685	-88.806	121992399600	Williamson	IL	15 - 18	138 - 178	Carbondale	Dekoven
Weatherford	37.967	-89.412	121452892900	Perry	IL	15 - 17	140 - 170	Tradewater	Davis
						25 - 27	237 - 266.5	Carbondale	Murphsyboro

1.2 CORE DESCRIPTION

The Brush Creek Quarry core was characterized from 202 to 221 ft and from 231 to 262 ft representing strata in the Mattoon formation around the Opdyke and Cohn coal seams. Figure 2 highlights the stratigraphy in detail as described by John Nelson and Scott Elrick, a detailed description can be found on the Illinois State Geological Survey(ISGS) Brush Creek Quarry Well page (Nelson and Elrick, 2010). Core photos from the characterized section are found in Figure 3.

The E. Miller/Hanna City core was characterized from 103 to 132 ft, 141.5 to 160.1 ft, 207.2 to 262.5ft, and 310.6 to 339 ft representing strata from the Shelburn and Carbondale formations around the Danville, Herrin, Springfield, Houchin Creek, and Colchester coal seams. Figure 4 highlights the stratigraphy in detail as described by John Nelson and Scott Elrick of the ISGS, a detailed description can be found on the ISGS E. Miller/ Hanna City Well page (Nelson and Elrick, 2012). Core photos from the characterized section are found in Figure 5 and Figure 6.

The Morris Well core was characterized from 138 to 178 ft, representing strata from the Carbondale Formation around the Dekoven coal seam. Figure 7 is a stratigraphic column by John Nelson of the ISGS, showing the cored intervals of the Morris Well. A detailed description can be found on the ISGS Morris Well page (Nelson, 2004). Core photos from the characterized section are found in Figure 8.

Weatherford Well core was characterized from 140 to 170 ft and 237 to 266.5 ft representing strata from the base of the Carbondale and Tradewater Formation around the Davis and Murphsyboro coal seams. Figure 9 is a stratigraphic column by Brett Denny of the ISGS, showing the cored intervals of the Weatherford Well, a detailed description can also be found on the ISGS Weatherford Well page (Denny, 2005). Core photos from the characterized section are found in Figure 10 and Figure 11.

Brush Creek Quarry:

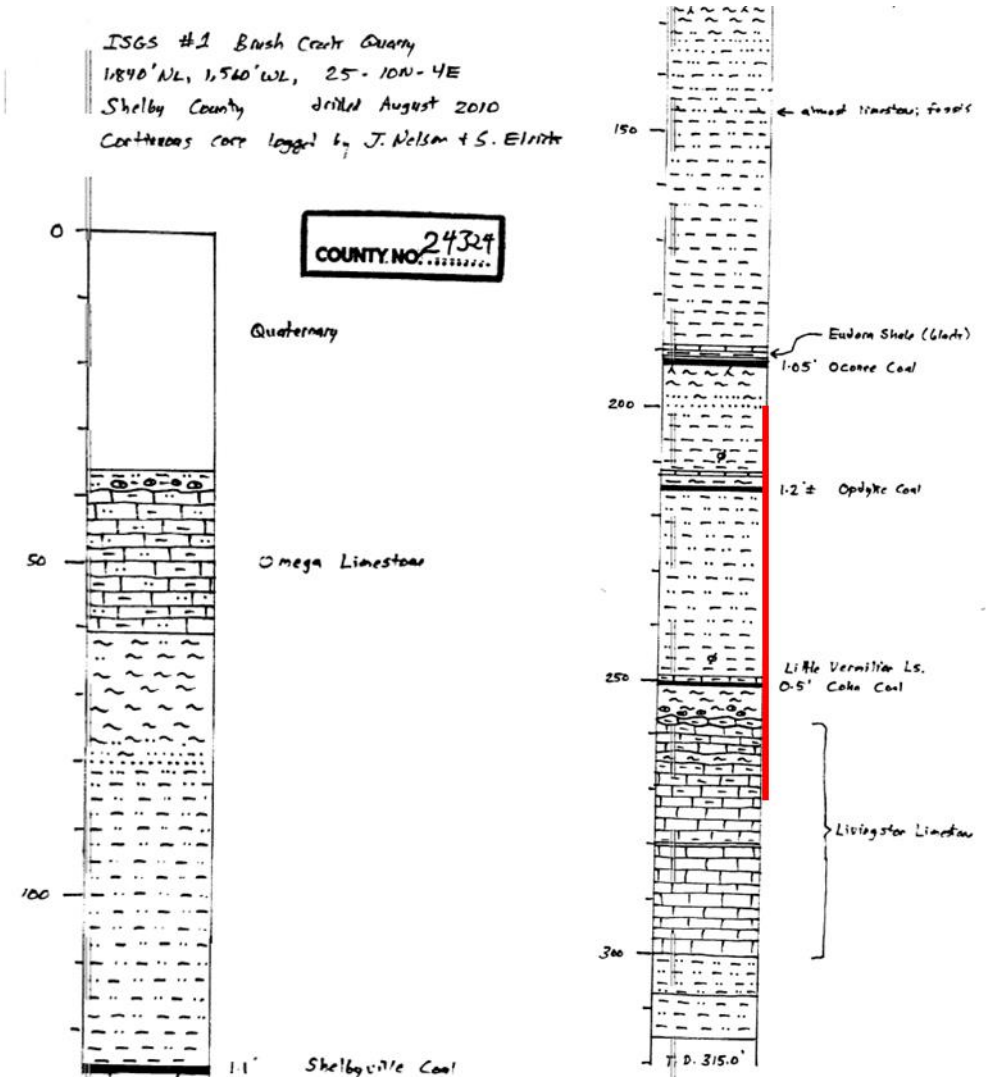

Figure 2: Detailed stratigraphic description of the Brush Creek Quarry Well by J. Nelson and S. Elrick; the red line represents the strata characterized in this report (Modified from Nelson and Elrick, 2010).

202–211 ft

211–221 ft

231–241 ft

241–251.5 ft

251.5–261 ft

Figure 3: Core photos of the characterized section in the Brush Creek Quarry Well from 202–211 ft and 231–261 ft.

E. Miller Hanna City Well:

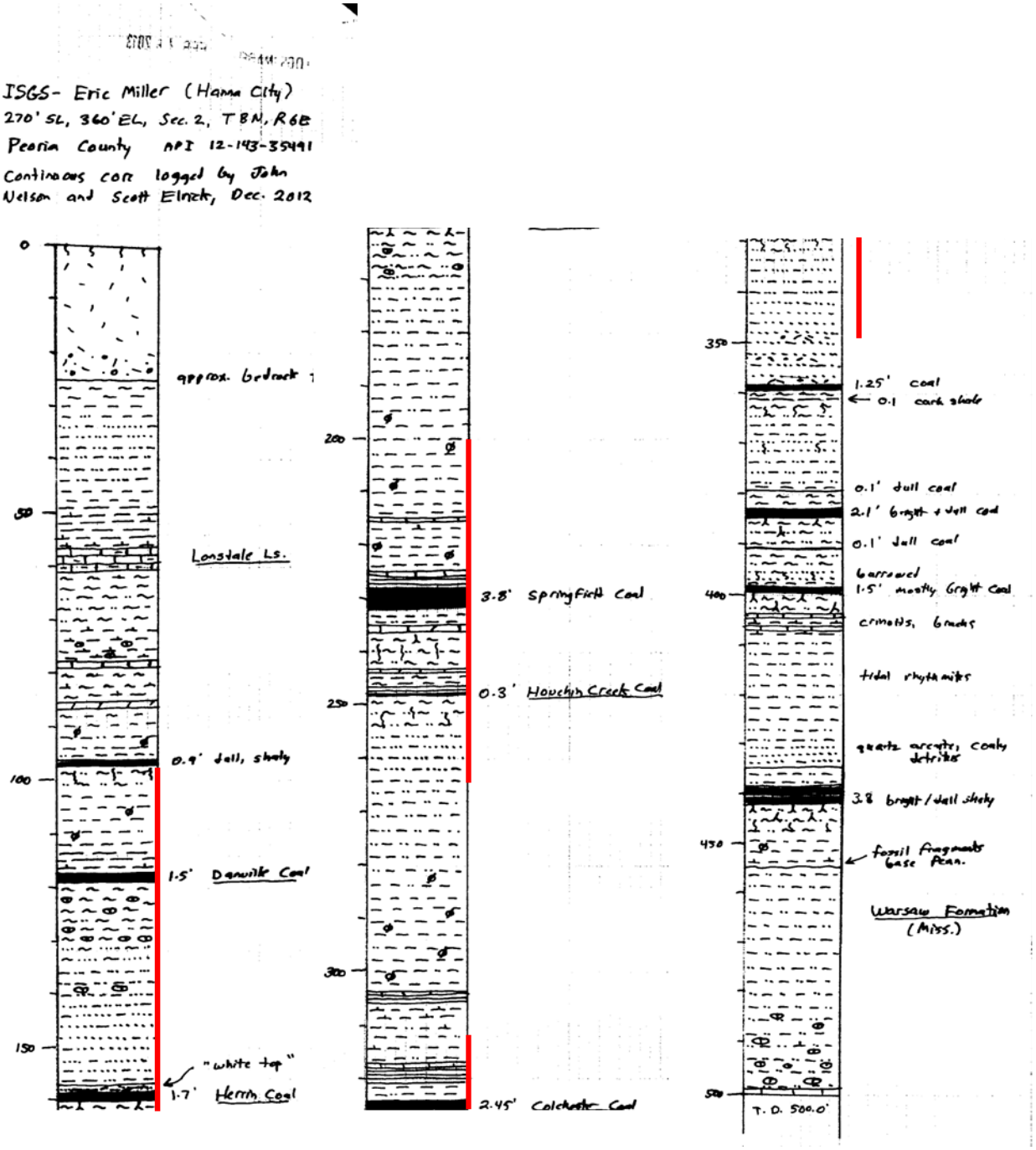

Figure 4: Detailed stratigraphic description of the E. Miller/Hanna City Well by J. Nelson and S. Elrick; the red lines represent the strata characterized in this report (Modified from Nelson and Elrick, 2012).

103–113 ft

113–123 ft

123–132 ft

141.5–150.8 ft

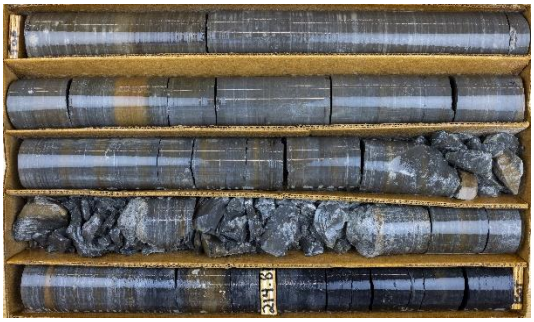

207.2–215.7 ft

215.7–225.3 ft

225.3–234.4 ft

234.4–243.9 ft

Figure 5: Core photos of the characterized section in the E. Miller/Hanna City Well from 103–132 ft, 141.5–150.8 ft, and 2017.2–243.9 ft.

243.9–253.1 ft

253.1–262.5 ft

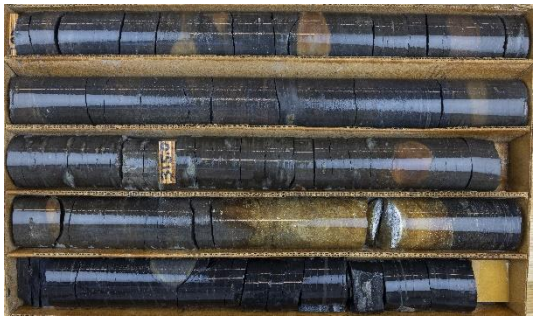

310.6–319.8 ft

319.8–329 ft

329–339.1 ft

Figure 6: Core photos of the characterized section in the E. Miller/Hanna City Well from 243.9–262.5 ft and 310.6–339.1 ft.

Morris Well:

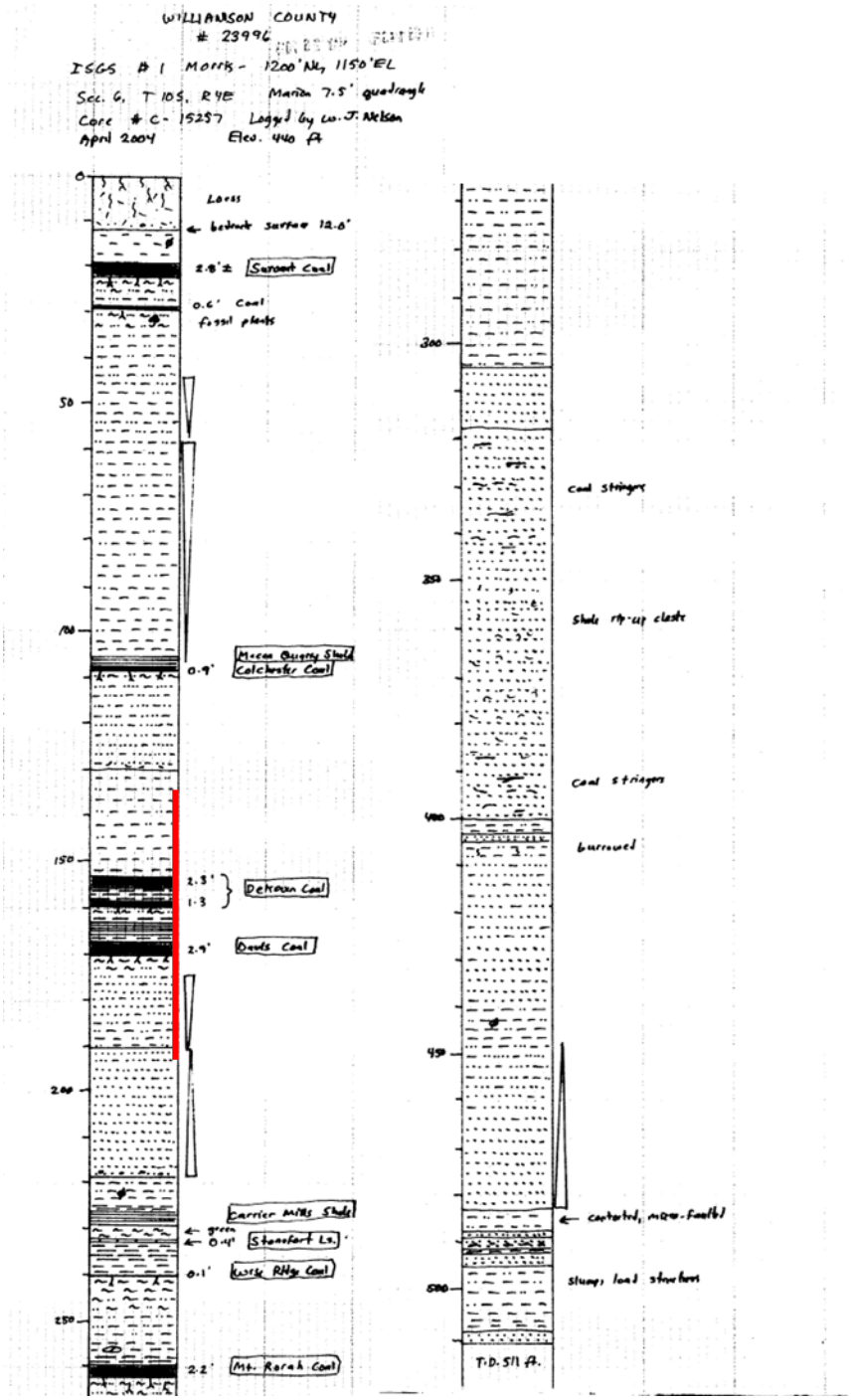

Figure 7: Detailed stratigraphic description of the Morris Well by J. Nelson; the red line represents the strata characterized in this report (Modified from Nelson, 2004).

138–148 ft

148–158 ft

158–168 ft

168–178 ft

Figure 8: Core photos of the characterized section in the Morris Well from 138–178 ft.

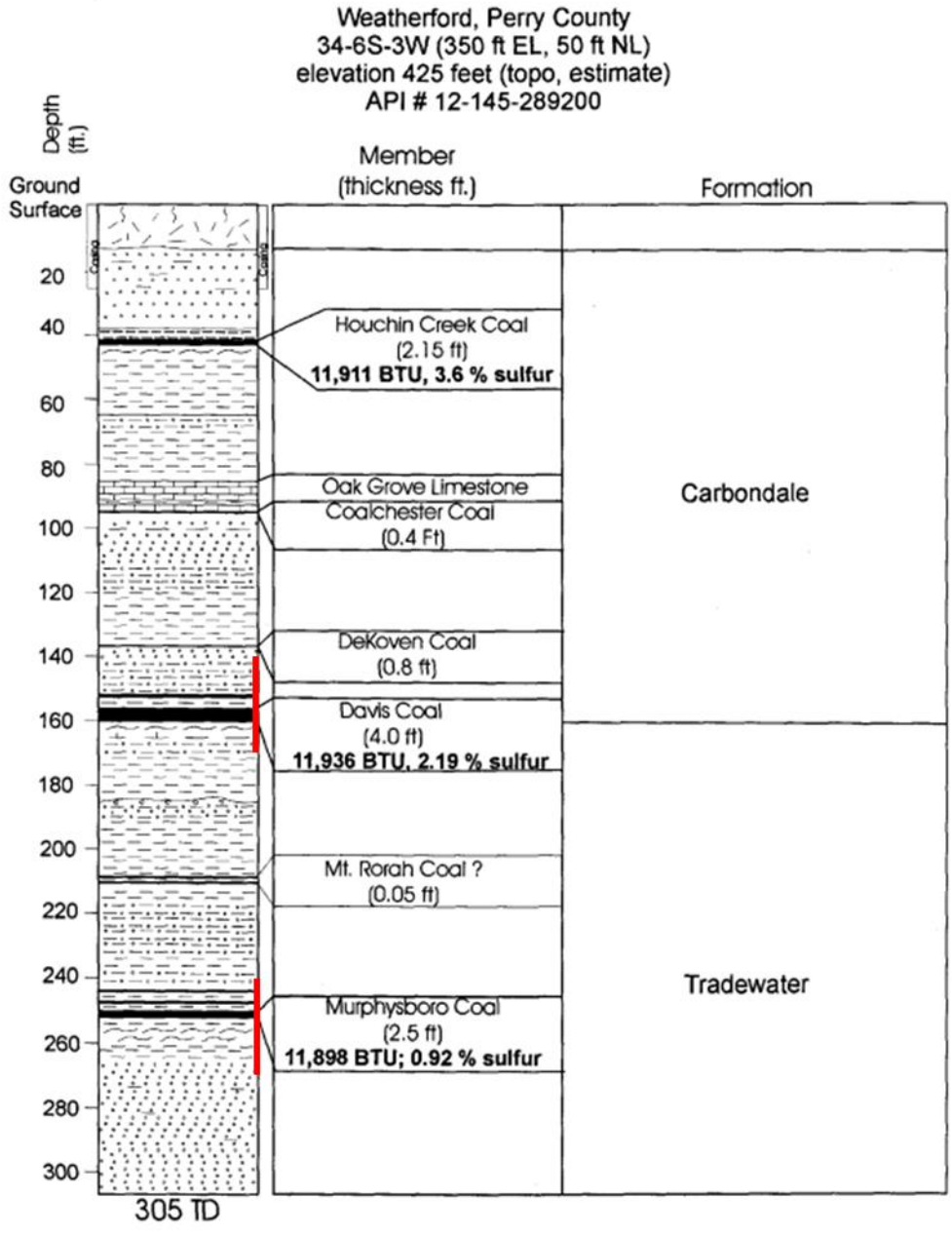

Figure 9: Detailed stratigraphic description of the Weatherford Well by B. Denny; the red lines represent the strata characterized in this report (Modified from Denny, 2005).

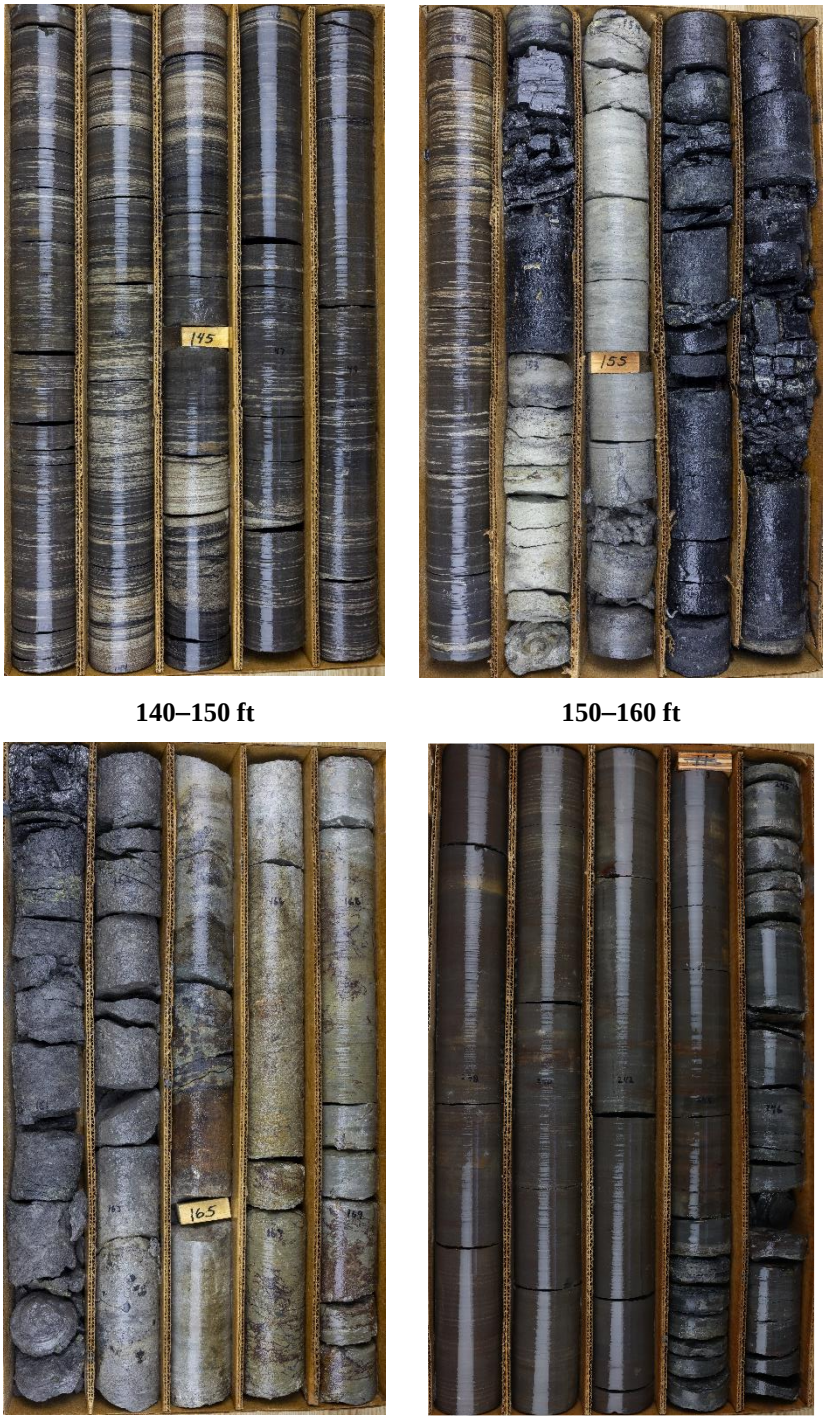

140–150 ft **150–160 ft**

160–170 ft **237–247 ft**

Figure 10: Core photos of the characterized section in the Weatherford Well from 140–170 ft and 237–247 ft.

247–256.5 ft **256.5–266.5 ft**

Figure 11: Core photos of the characterized section in the Weatherford Well from 247–266.5 ft.

2. DATA ACQUISITION AND METHODOLOGY

The core was evaluated using medical CT scanning and high spatial resolution geophysical measurements along its length, including X-ray fluorescence (XRF) spectrometry.

2.1 MEDICAL CT SCANNING

Core scale CT scanning was performed with a Toshiba Aquilion TSX-101A/R medical CT scanner shown in Figure 12. The medical CT scanner generates images with a resolution in the millimeter range, with scans having voxel resolutions of 0.43 x 0.43 mm in the XY plane and 0.50 mm along the core's long axis (i.e., z-axis). The scans were conducted at a voltage of 135 kV and at a current of 200 mA. Subsequent processing and combining of stacks were performed to create three-dimensional (3D) volumetric representations of the cores and a two-dimensional (2D) cross-section through the middle of the core samples using ImageJ, an open-source image processing software package (Schneider et al., 2012). The variation in greyscale values observed in the CT images indicates changes in the CT number (CTN) obtained from the CT scans, which is directly proportional to changes in the attenuation and density of the scanned rock; darker regions are less dense. Filled fractures, open fractures, and changes in bedding structure can all be resolved via careful examination of the CT images (Figures 16–30). While the medical CT scanner was not used for detailed characterization in this study, it allowed for non-destructive bulk characterization of the core.

Figure 12: Toshiba Aquilion Multislice Helical CT scanner at NETL used for core analysis.

2.2 INDUSTRIAL CT SCANNING

High-resolution CT scans were performed on intervals of interest using NETL's North Star Imaging Inc. M-5000® Industrial CT System (Figure 13). The system is used to obtain higher resolution scans, resolving some unclear features from the medical scans. NETL's North Star Imaging Inc. M-5000® was used to obtain 2D radiographs of the samples 1,440 times while rotating 360°, or at every 0.25°. Radiographs were comprised of 10 images averaged with a 5 s acquisition for each image to ensure sufficient image contrast.

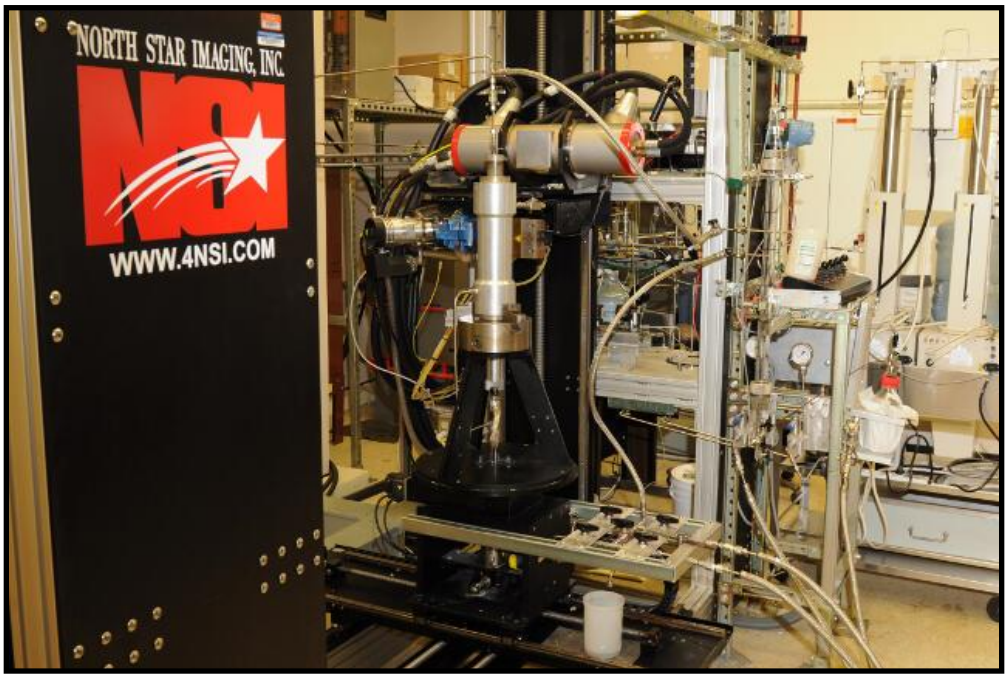

Figure 13: North Star Imaging Inc. M-5000 ® Industrial CT Scanner at NETL used for core analysis.

2.3 CORE LOGGING

Geophysical measurements of magnetic susceptibility and attenuated gamma counts were obtained with a Geotek® MSCL system on competent sections of the cored intervals and are reported in Section 3.4. Additionally, the system measured bulk elemental chemistry using a built-in, portable XRF spectrometer. The compiled core logs were scaled to fit on single pages for rapid review of the combined data from the medical CT scans and XRF readings.

2.3.1 Magnetic Susceptibility

Magnetic susceptibility is a measure of the degree of magnetization in a sample. The sample is exposed to an external magnetic field and magnetic susceptibility is its measured magnetic response to that field:

$$J = kH$$

Where, J is the magnetic response (per unit volume), k is volume susceptibility, and H is an external magnetic field. The measurement unit is dimensionless (abbreviated as SI).

All materials have magnetic susceptibility. Positive values of magnetic susceptibility indicate that materials are *paramagnetic* and occur in rocks that consist of the majority ferromagnetic, ferrimagnetic, or antimagnetic (iron-bearing) materials. Negative values of magnetic susceptibility indicate that materials are *diamagnetic* and occur in rocks dominated by non-iron material (e.g., calcite or quartz). Table 2 lists examples of common magnetic susceptibility ranges (Hunts et al., 1995).

Magnetic susceptibility was measured using the Bartington point sensor, where a 1-cm diameter, low intensity (8.0 A/m RMS), non-sensitive, alternating magnetic field (2 kHz) was generated for 10 s. To minimize any potential drift in the oscillating field, the point sensor was zeroed at the beginning and end of the sample and after every fifth measurement. The point sensor, due to the small field, was limited in whole core measurements and was temperature dependent (Geotek Ltd. Multi-Sensor Core Logger Manual, Version 05-10; Geotek Ltd., 2010).

Table 2: Magnetic Susceptibility Values for Common Minerals (Hunts et al., 1995)

Mineral	x (*10^{-6}) SI
Water	9
Calcite	-7.5 to -39
Halite, Gypsum	-10 to -60
Shale	63 to 18,600
Illite, Montmorillonite	330 to 410
Pyrite	5 to 3,500
Chalcopyrite	23 to 400
Hematite	500 to 40,000
Magnetite	1,000,000 to 5,700,000

2.3.2 Gamma Density

Gamma density was acquired by subjecting the sample to gamma radiation and then measuring the attenuation of that radiation. The attenuation is directly proportional to the density of the sample and is acquired by measuring the difference between radiation energy at the emission source and after it passes through the sample. Specifically, the MSCL software calculates the bulk density, ρ, by using the following equation:

$$\rho = \left(\frac{1}{\mu d}\right) \ln\left(\frac{I_o}{I}\right)$$

Where μ = Compton attenuation coefficient, d = sample thickness, I_o = source intensity, and I = measured intensity.

2.3.3 XRF Spectrometry

In addition to the geophysical measurements, a portable handheld Olympus Vanta M Series XRF Spectrometer was used to measure relative elemental abundances of aggregated "light elements" up to and including sodium, and various "heavy elements" which were measured individually. Elemental abundances are reported in ppm relative to the total elemental composition (i.e., the total XRF counts).

The XRF spectrometer measures elemental abundances by subjecting the sample to X-ray photons. The high energy of the photons displaces inner orbital electrons in the respective elements. The vacancies in the lower orbitals cause outer orbital electrons to "fall" into lower orbits to satisfy the disturbed electron configuration. The substitution into lower orbitals causes a release of a secondary X-ray photon, which has an energy associated with a specific element. These relative and element specific energy emissions can then be used to determine bulk elemental composition.

The Olympus Vanta M Series XRF Spectrometer used a "GeoChem(3-beam) Mode" to run at 30.48 cm (1 ft) resolution for 120 s exposure time analysis (40 s per beam). The GeoChem(3-beam) Mode utilizes a 3-beam analysis that resolves major (Mg, Al, Si, P, S, Fe, K, Ca, and Ti), minor (V, Cu, Ni, Cr, Mn, Ba, Sr, and Pb), and trace elements (Co, Zn, As, Zr, Mo, Ag, Cd, Sn, Sb, Hg, W, Th, U, and Bi), and some rare earth elements (Y, Ce, La, Pr, and Nd) (orange, Figure 14). The system also resolves an aggregated "light element" (H to Na) (green, Figure 14).

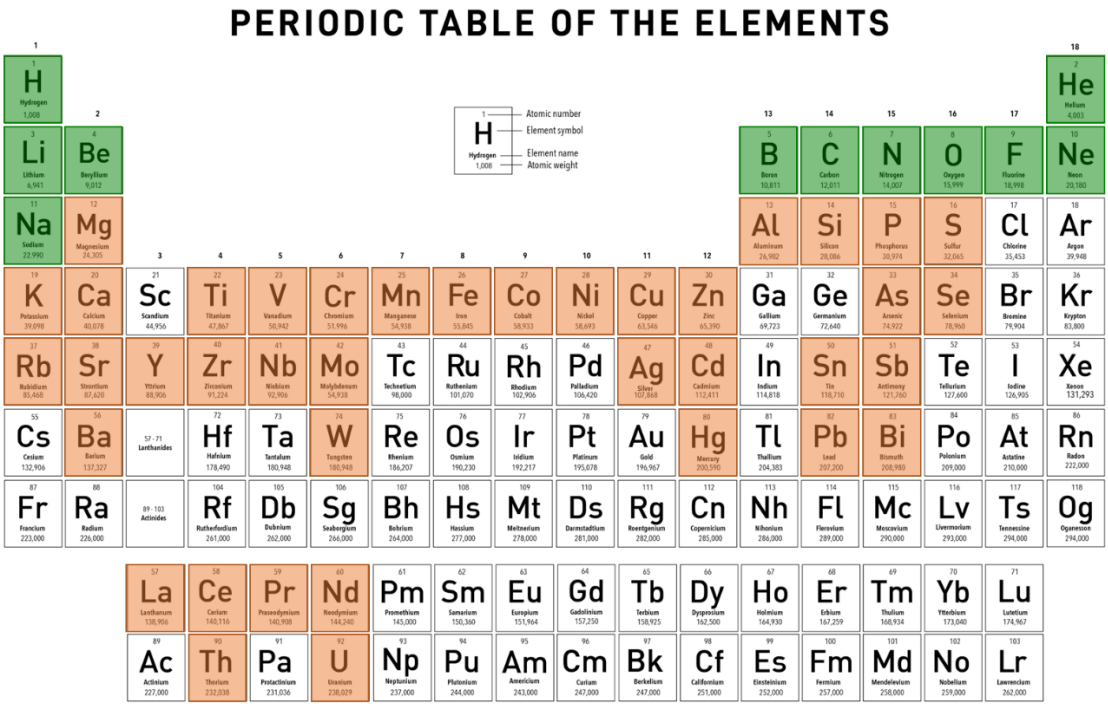

Figure 14: Periodic table showing elements measurable by the Olympus Vanta M Series XRF Spectrometer using the "GeoChem(3-beam)" mode.

2.4 DATA COMPILATION

Strater® by Golden Software was used to compile the medical CT data into a series of logs. The data used to generate these logs can be accessed from NETL's EDX online system using the following link: https://edx.netl.doe.gov/dataset/illinois-basin-coal-wells.

3. RESULTS

The following sections contain the data obtained from the medical and industrial CT scanners, in addition to the MSCL scans, of the cored intervals.

3.1 MEDICAL CT SCANS

Processed 2D slices of the medical CT scans through the cores are shown. As discussed previously, the variation in greyscale values observed in the medical CT images indicates changes in the CTN obtained, which is directly proportional to changes in the attenuation of the X-ray beam, and thus density of the scanned rock (i.e., darker regions are less dense, lighter regions are denser).

3.1.1 XZ Planes

A 2D image through the center of each core can be found in Figure 16 through Figure 30. These are referred to as "XZ" planes with the coordinates that are shown in Figure 15. Each image has a red 2-cm scale bar; the core diameter is 2.5 in. (10.16 cm). The labels below each 2D XZ plane in Figure 16 through Figure 30 are the depth of each core. Due to the contrast difference between the coal seams and the surrounding rock two images of each section are shown. The images on the left have a CTN greyscale from 1,000 to 4,500 to show variation in the rock surrounding the coal seams. The images on the right have a CTN greyscale from -1,600 to 4,500 to visualize the less dense coals (Figure 16).

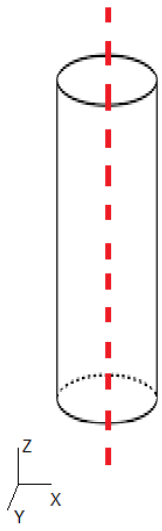

Figure 15: Schematic of the XZ isolated plane through the vertical center of the medical CT scans.

Left: CTN Greyscale from 1,000 to 4,500 to highlight rock features

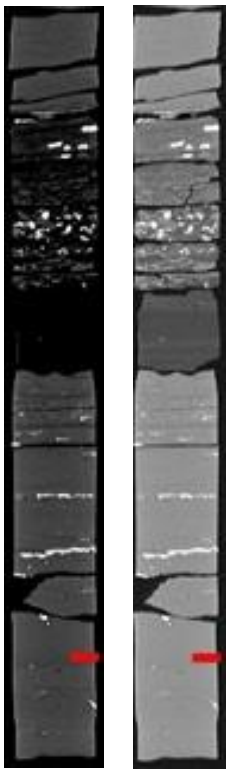

Right: CTN Greyscale from -1,600 to 4,500 to highlight coal features

Figure 16: Greyscale variations in medical CT images; images on the left are CTN greyscale from 1,000 to 4,500 to highlight rock features and images on the right are CTN greyscale from -1,600 to 4,500 to highlight coal features.

3.1.2 Brush Creek Quarry Well

Figure 17: 2D isolated planes through the vertical center of the medical CT scans of the Brush Creek Quarry Well from 202–221 ft.

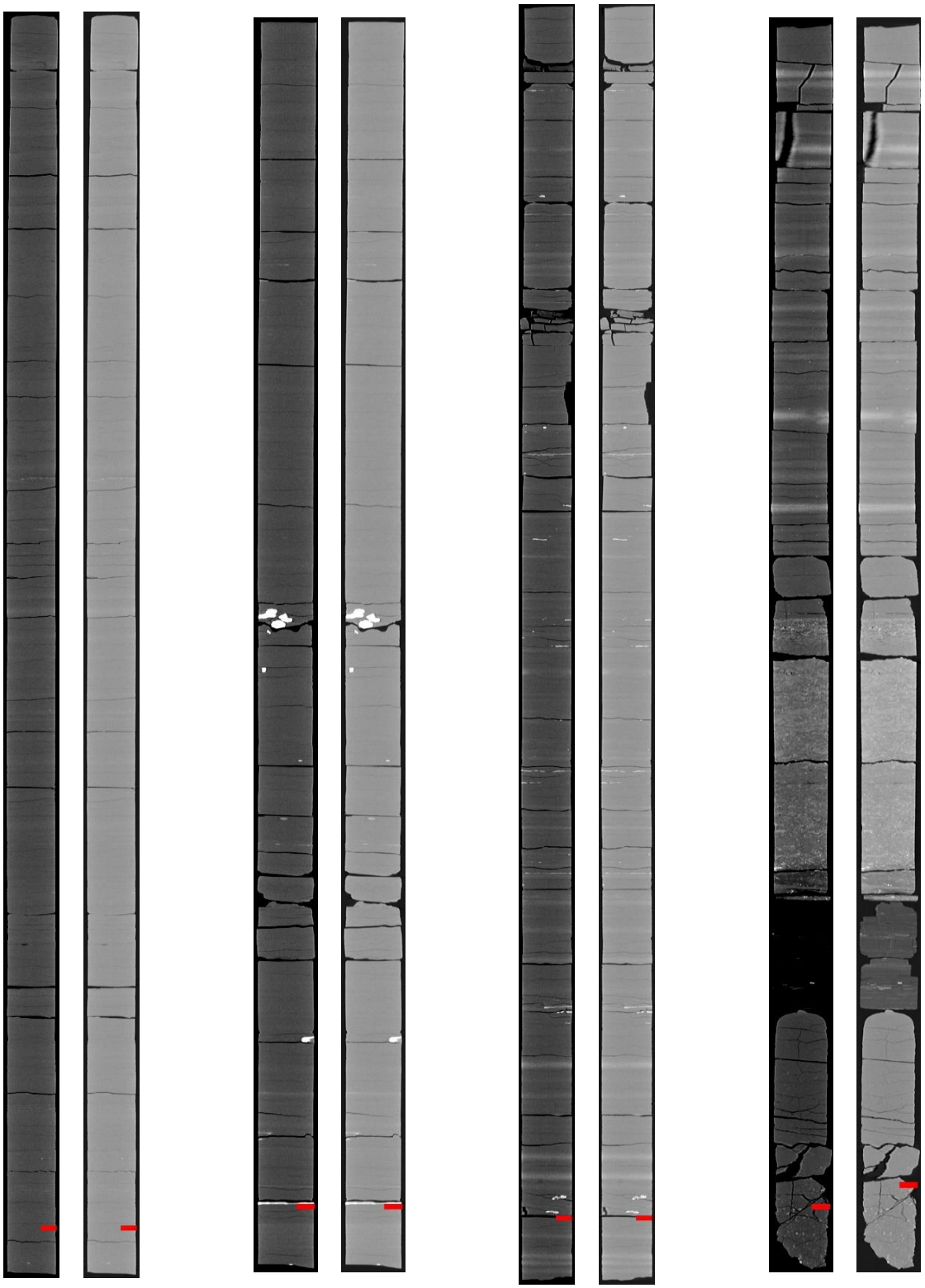

231–237 ft 237–241 ft 242–247 ft 247–251 ft

Figure 18: 2D isolated planes through the vertical center of the medical CT scans of the Brush Creek Quarry Well from 231–251 ft.

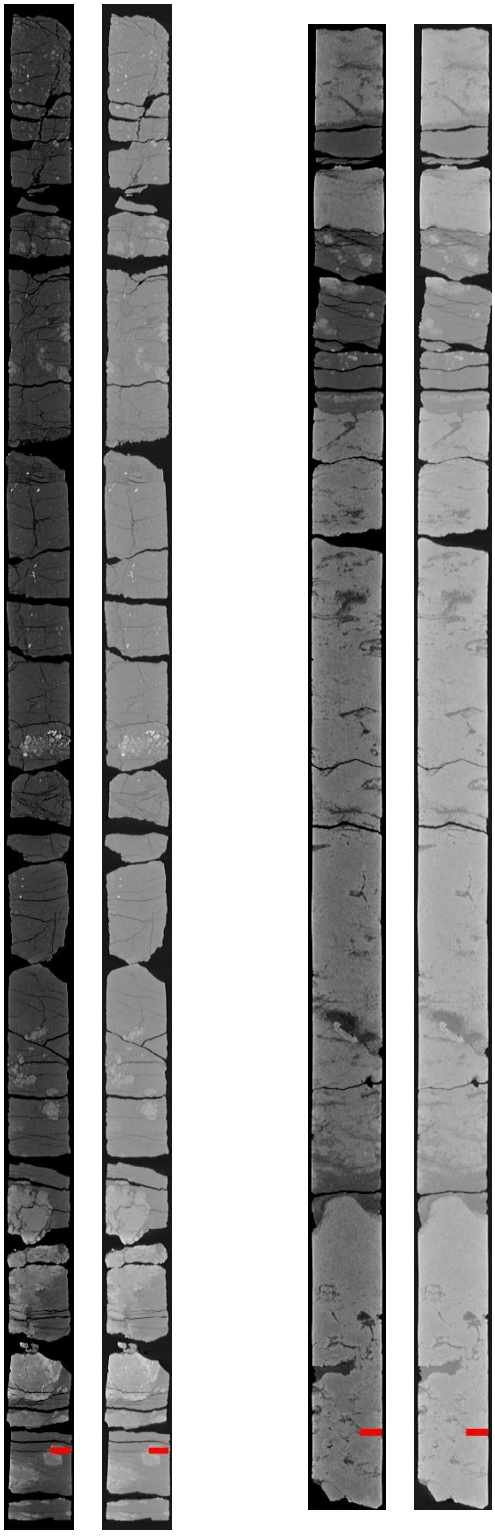

251–256 ft **256–261 ft**

Figure 19: 2D isolated planes through the vertical center of the medical CT scans of the Brush Creek Quarry Well from 251–261 ft.

3.1.3 E. Miller/Hanna City Well

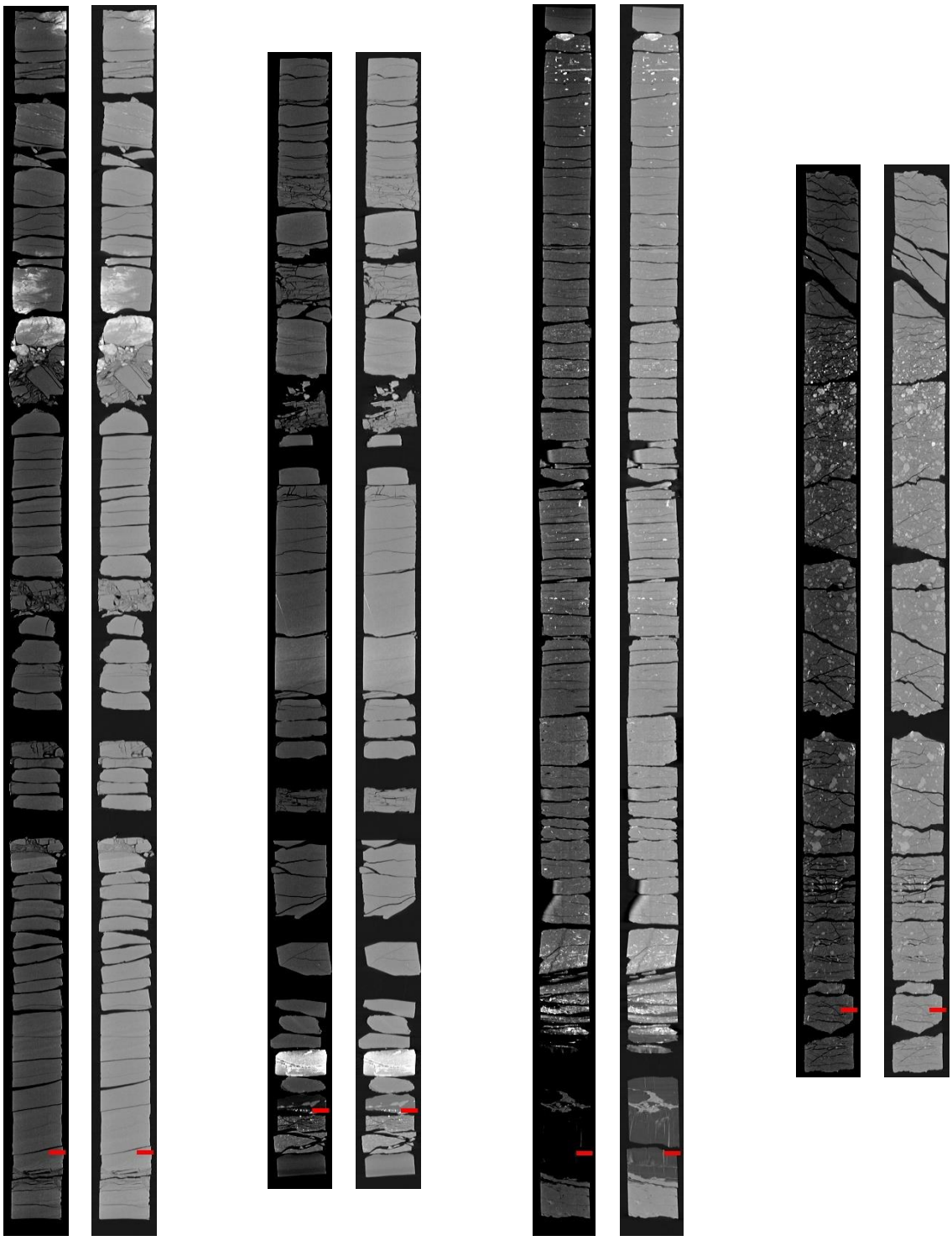

103–108 ft **108–113 ft** **113–119 ft** **119–123 ft**

Figure 20: 2D isolated planes through the vertical center of the medical CT scans of the E. Miller/Hanna City Well from 103–123 ft.

123–128 ft **128–132 ft** **142–147 ft** **147–151 ft**

Figure 21: 2D isolated planes through the vertical center of the medical CT scans of the E. Miller/Hanna City Well from 123–132 ft and 142–151 ft.

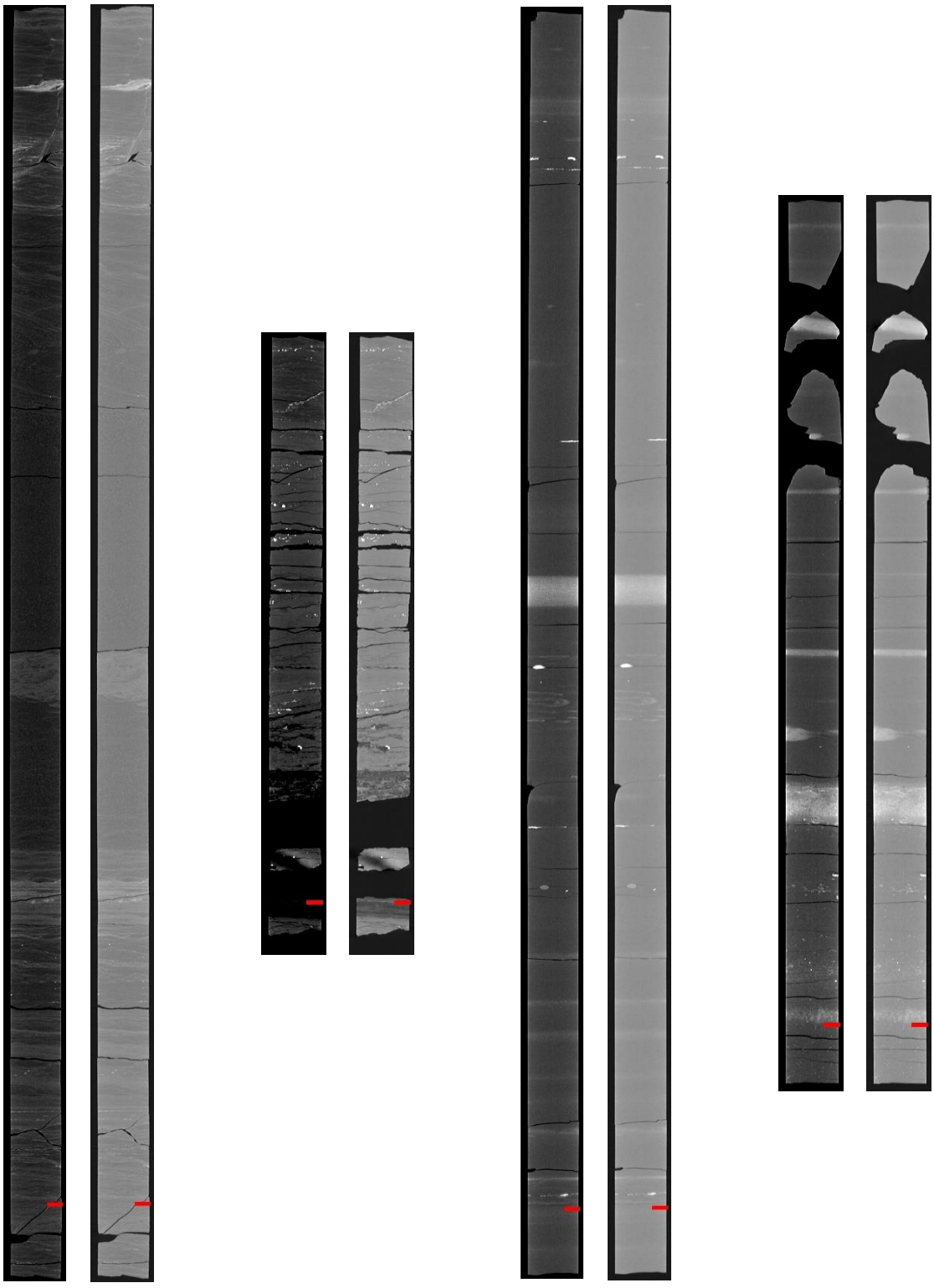

151–156 ft **156–160 ft** **207–212 ft** **212–216 ft**

Figure 22: 2D isolated planes through the vertical center of the medical CT scans of the E. Miller/Hanna City Well from 151–160 ft and 207–216 ft.

216–221 ft **221–225 ft** **225–230 ft** **230–234 ft**

Figure 23: 2D isolated planes through the vertical center of the medical CT scans of the E. Miller/Hanna City Well from 216–234 ft.

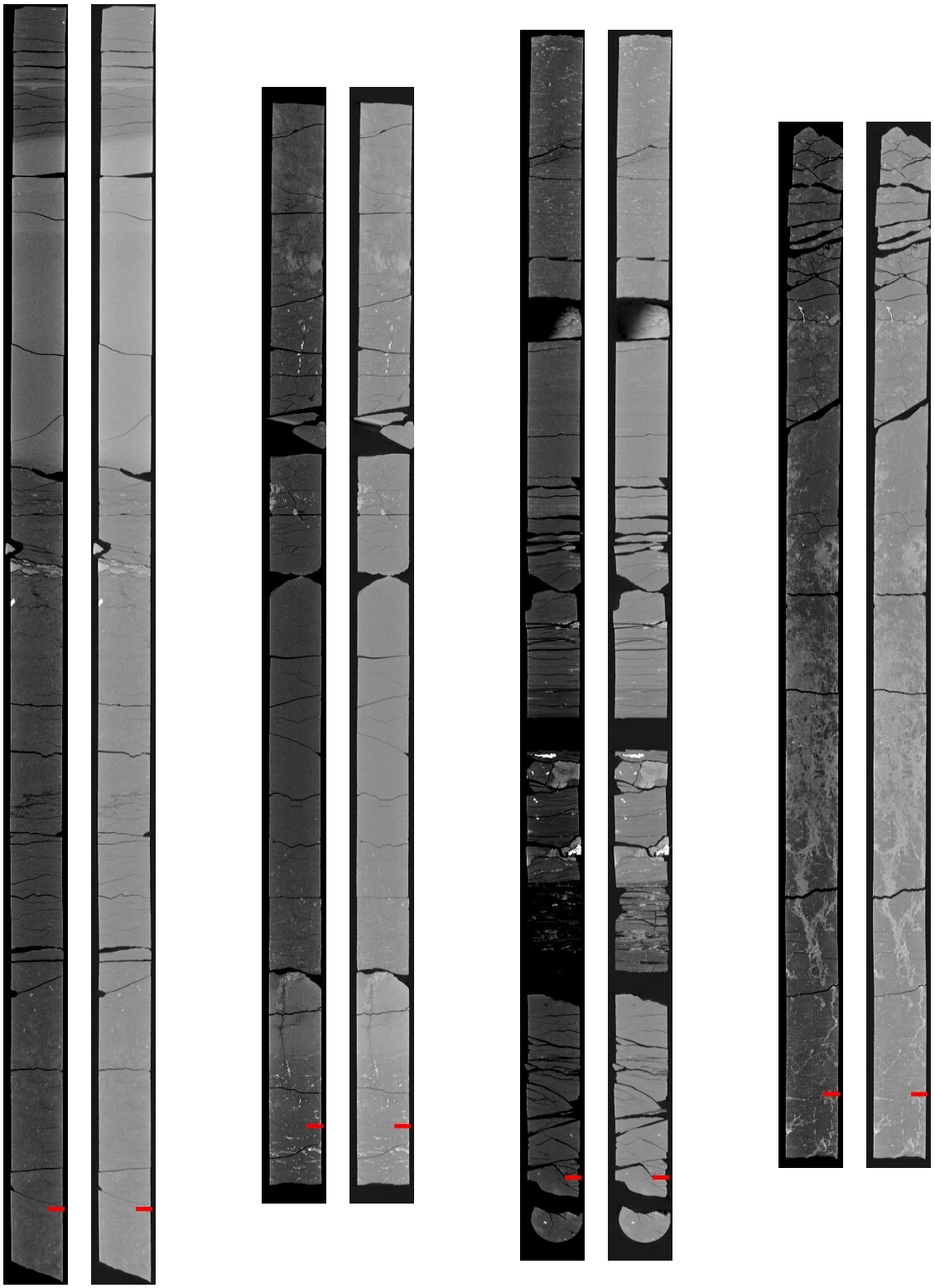

234–239 ft **239–244 ft** **244–249 ft** **249–253 ft**

Figure 24: 2D isolated planes through the vertical center of the medical CT scans of the E. Miller/Hanna City Well from 234–253 ft.

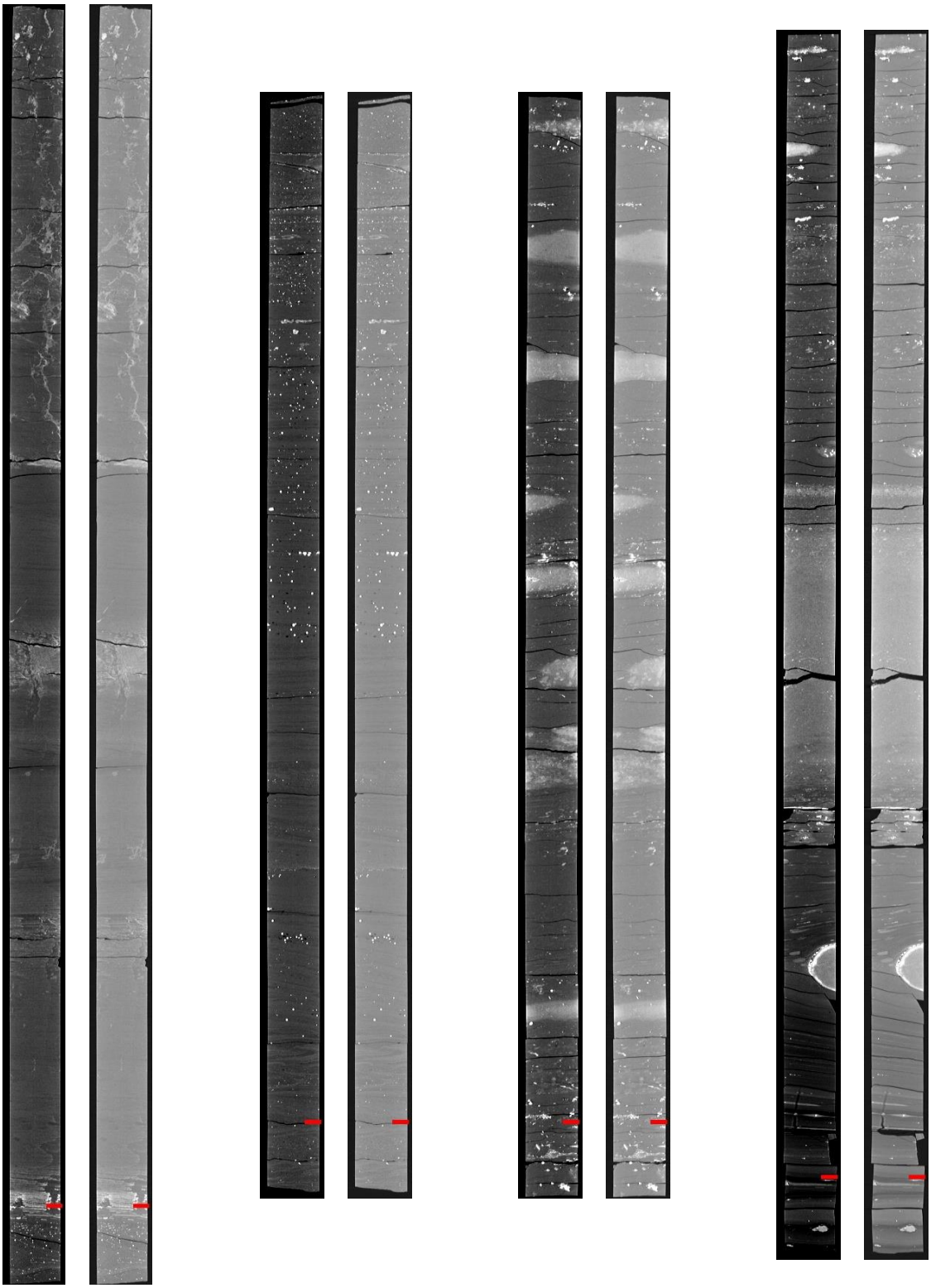

253–258 ft 258–263 ft 310–315 ft 315–320 ft

Figure 25: 2D isolated planes through the vertical center of the medical CT scans of the E. Miller/Hanna City Well from 253–263 ft and 310–320 ft.

320–325 ft 325–329 ft 329–334 ft 334–339 ft

Figure 26: 2D isolated planes through the vertical center of the medical CT scans of the E. Miller/Hanna City Well from 320–339 ft.

3.1.4 Morris Well

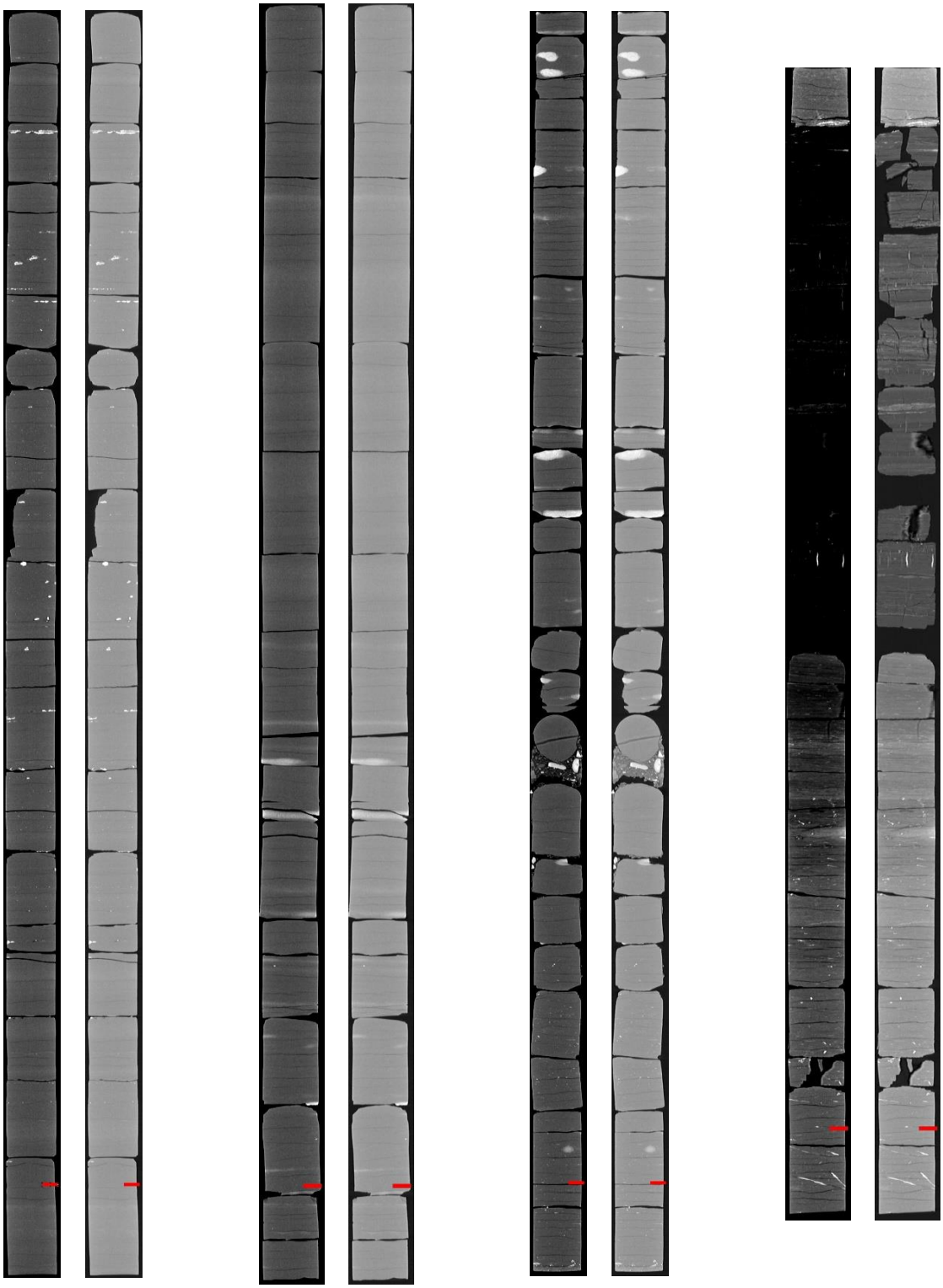

138–143 ft 143–148 ft 148–153 ft 153–158 ft

Figure 27: 2D isolated planes through the vertical center of the medical CT scans of the Morris Well from 138–158 ft.

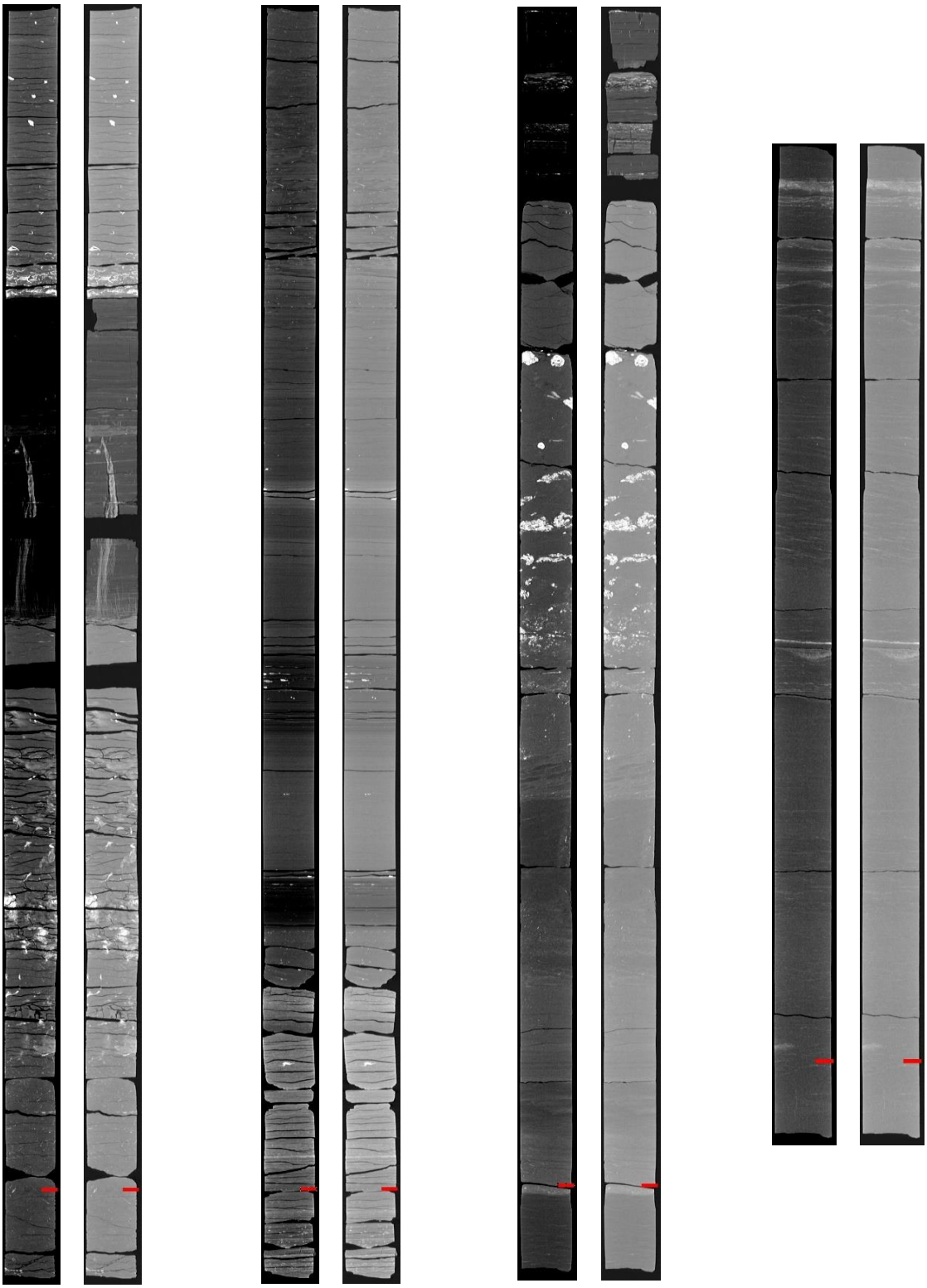

158–163 ft 163–168 ft 168–174 ft 174–178 ft

Figure 28: 2D isolated planes through the vertical center of the medical CT scans of the Morris Well from 158–178 ft.

3.1.5 Weatherford Well

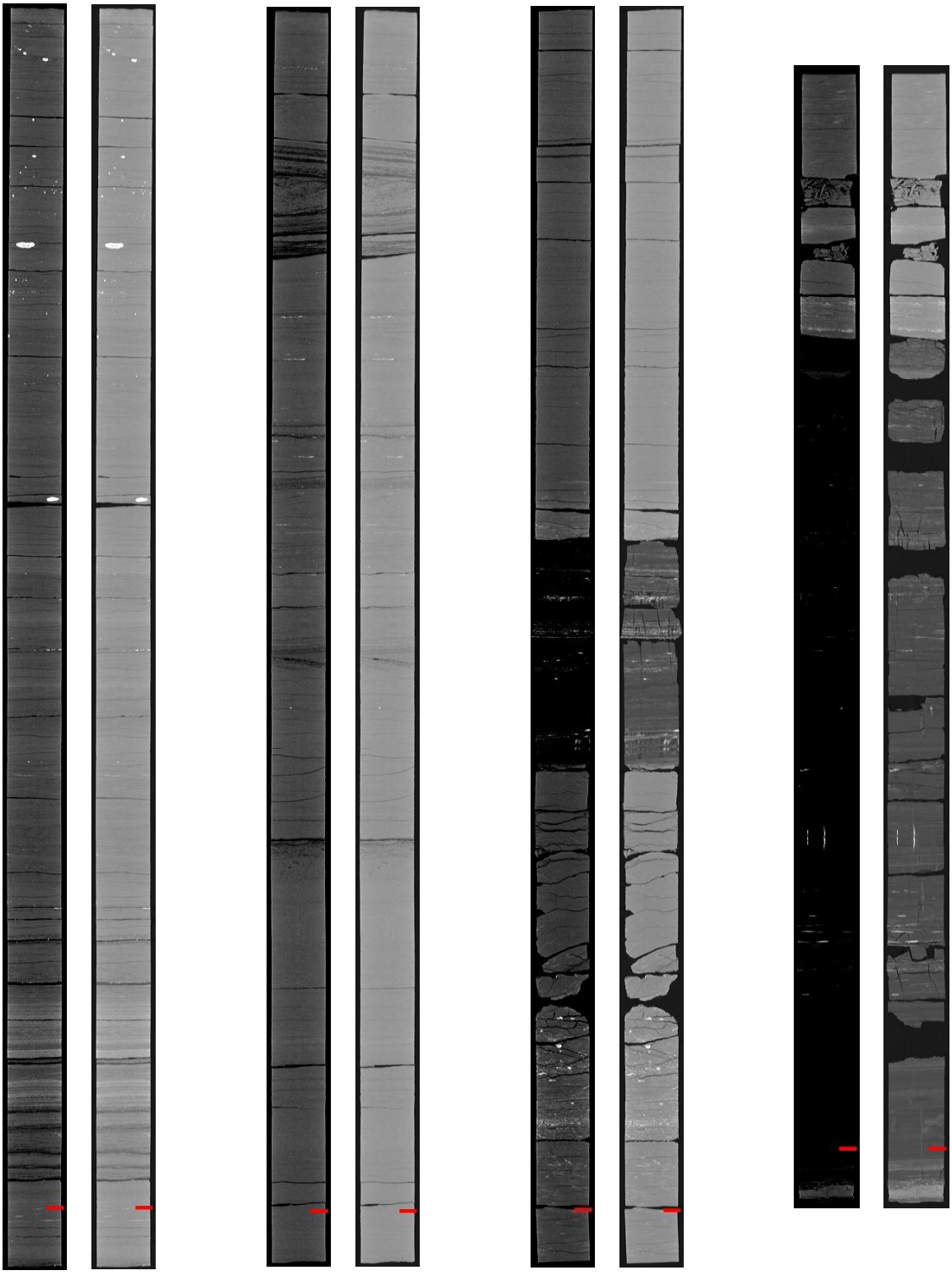

140–145 ft **145–150 ft** **150–155 ft** **155–160 ft**

Figure 29: 2D isolated planes through the vertical center of the medical CT scans of the Weatherford Well from 140–160 ft.

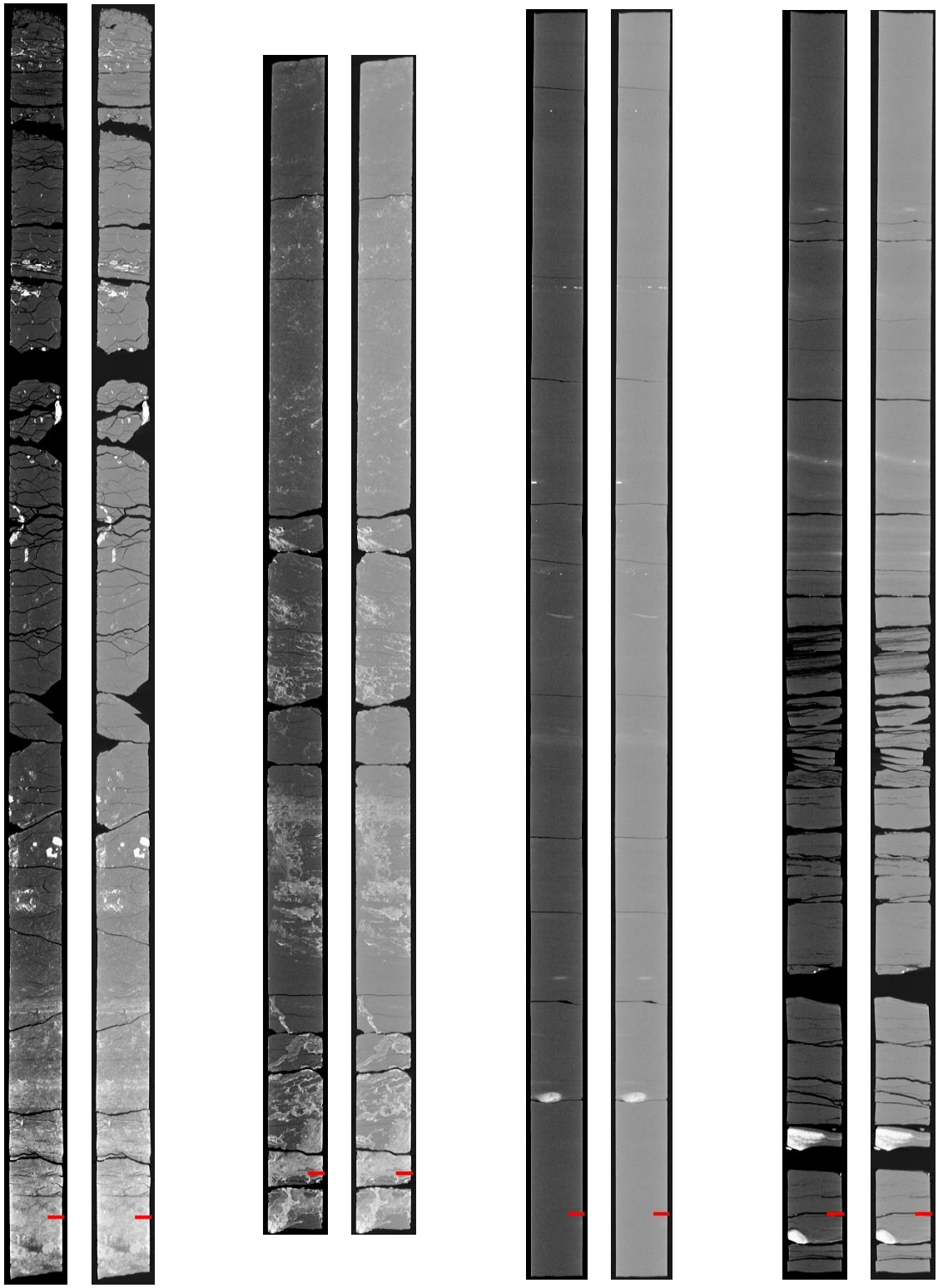

160–165 ft **165–170 ft** **237–242 ft** **242–247 ft**

Figure 30: 2D isolated planes through the vertical center of the medical CT scans of the Weatherford Well from 160–170 ft and 237–247 ft.

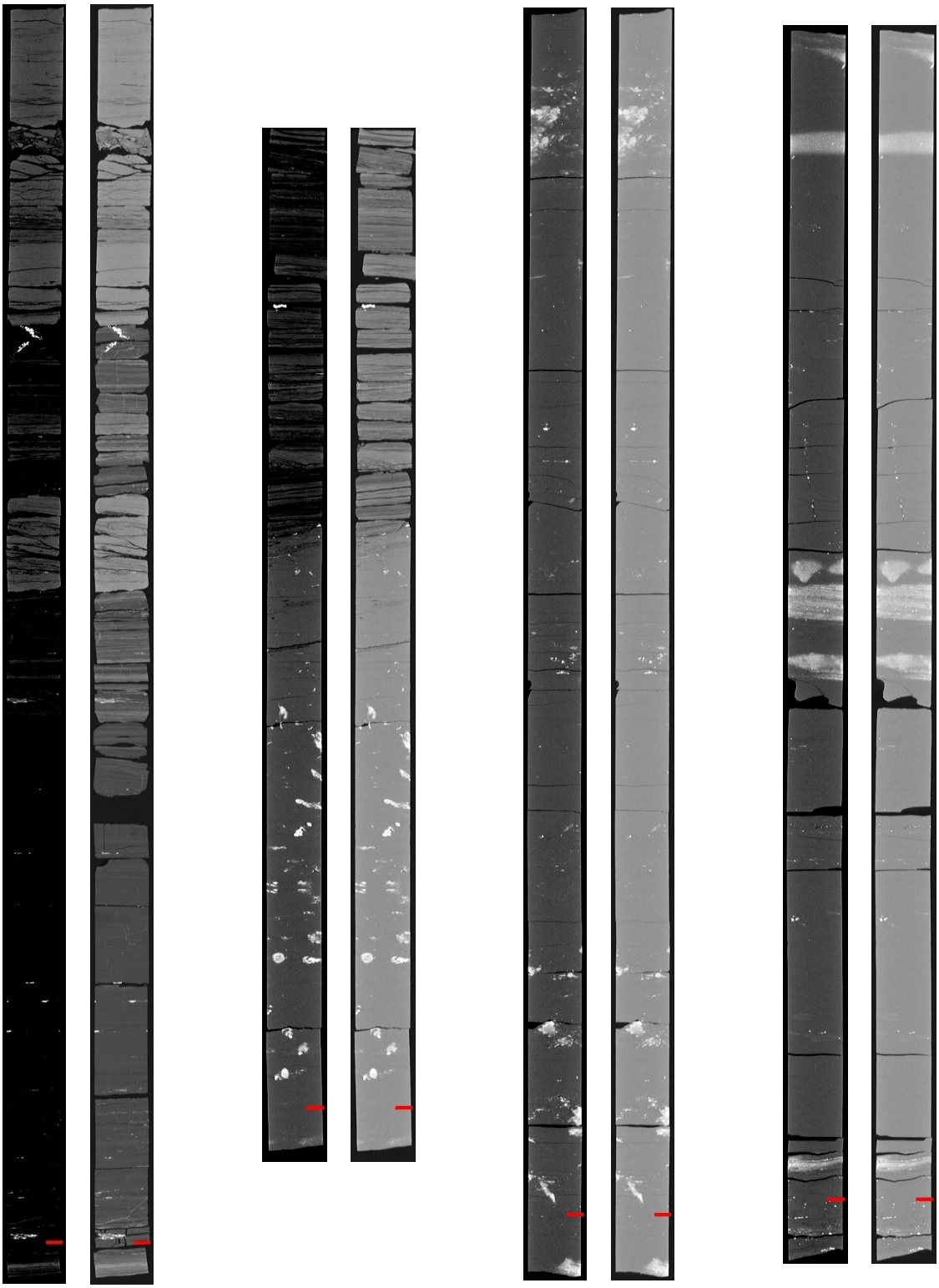

247–253 ft **253–256 ft** **256–262 ft** **262–266 ft**

Figure 31: 2D isolated planes through the vertical center of the medical CT scans of the Weatherford Well from 247–266 ft.

3.2 ADDITIONAL CT DATA

Additional CT data can be accessed from NETL's EDX online system using the following link: https://edx.netl.doe.gov/dataset/illinois-basin-coal-wells. The original CT data is available as 16-bit tif stacks suitable for reading with ImageJ (Schneider et al., 2012) or other image analysis software.

3.2.1 Medical CT Image Videos

In addition, videos showing the variation along the length of the cross-section images shown in the previous section are available for download and viewing on EDX. A single image from these videos is shown in Figure 31, where the cross-section of E. Miller/Hanna City Well core from 147–151 ft displays soft sediment deformation. The videos on EDX show this XY variation along the entire length of the core.

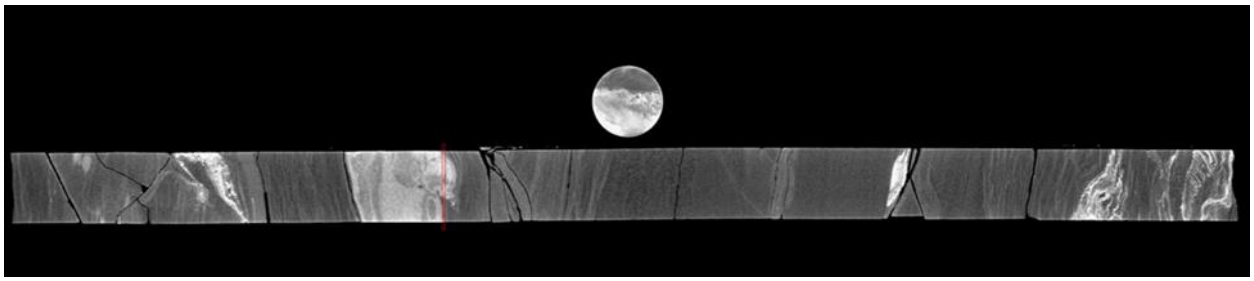

Figure 32: Single image from a video file available on EDX showing variation in the E. Miller/Hanna City Well core from 147–151 ft. Image above shows the variation in composition within the matrix perpendicular to the core length. The red line through the XZ-plane image of the core shows the location of the XY-plane displayed above.

3.2.2 Industrial CT Scans

Detailed industrial CT scans of core sections were performed at NETL. The industrial CT scanner was used to obtain higher resolution images with a voxel resolution of 36.8 μm^3 and capture the details of internal features clearly. There was one scan taken in the Weatherford Well at 254 ft. An XZ reslice of images through the center of this scan is shown in Figure 32. The 16-bit and rescale 8-bit tif stacks are available on EDX.

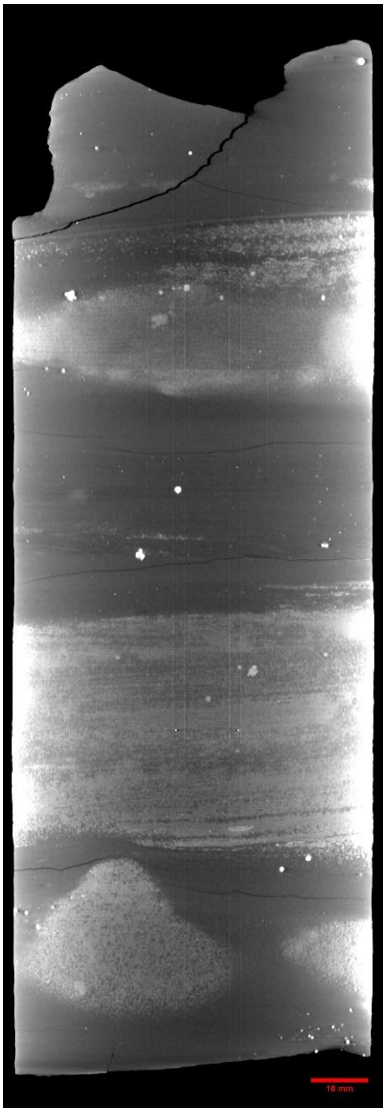

Figure 33: Weatherford Well industrial CT scanner images from 264 ft, scale bar is 1 cm (10 mm).

3.3 DUAL ENERGY CT SCANNING

Dual energy CT scanning uses two sets of images, produced at different X-ray energies, to approximate the density (ρ_B) (Siddiqui and Khamees, 2004; Johnson, 2012). The technique relies on the use of several standards of known ρ_B to be scanned at the same energies as the specimen. These scans are performed at lower energies (<100 KeV) and higher energies (>100 KeV) to induce two types of photon interactions with the object (Figure 33). The lower energy scans induce photoelectric absorption, which occurs when the energy of the photon is completely absorbed by the object mass and causes ejection of an outer orbital electron (Figure 33a). The high energy scans induce Compton scattering, which causes a secondary emission of a lower

energy photon due to incomplete absorption of the photon energy in addition to an electron ejection (Figure 33b).

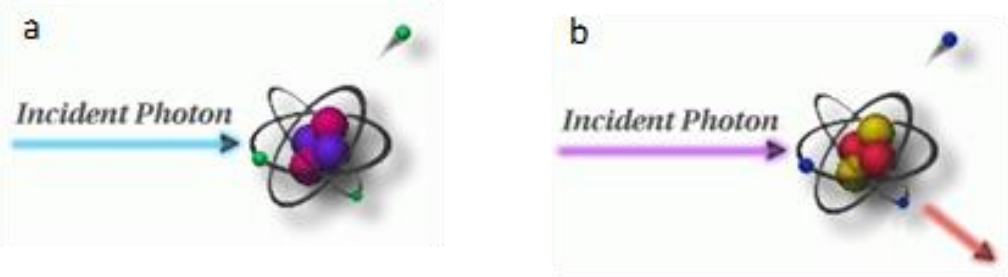

Figure 34: Photon interactions at varying energies: a) Photoelectric absorption, b) Compton scattering. Modified from Iowa State University Center for Nondestructive Evaluation (2021).

Medical grade CT scanners are typically calibrated to known standards, with the output being translated in CTN or Hounsfield Units (HU). Convention for HU defines water as 0 and air as -1,000. A linear transform of recorded HU values is performed to convert them into CTN. This study used CTN as it is the native export format for the medical CT scanner, but it is possible to use HU. Dual energy CT requires at least three calibration points, and it is prudent to utilize standards that approximate the object or material of interest. Pure samples of aluminum, graphite, and sodium chloride were used as the calibration standards as they most closely approximate the rocks and minerals of interest (Table 3). Most materials denser than water or with higher atomic masses have a non-linear response to differing CT energies (Table 4).

Table 3: Dual Energy Calibration Standards, Bulk Density (gm/cm^3)

Material	ρ_B (g/cm^3)
Air	-0.001
Water	1
Graphite	2.3
Sodium Chloride	2.16
Aluminum	2.7

Table 4: Dual Energy Calibration Standards, HU and CTN for "Low" and "High" Energies

Material	HU		CTN	
	80 KeV	135 KeV	80 KeV	135 KeV
Air	-993	-994	31,775	31,774
Water	-3.56	-2.09	32,764	32,766
Graphite	381	437	33,149	33,205
Sodium Chloride	1,846	1,237	34,614	34,005
Aluminum	2,683	2,025	35,451	34,793

Dual energy CT utilizes these differences to calibrate to the X-ray spectra. Two equations with three unknowns each are utilized to find ρ_B (Siddiqui and Khamees, 2004):

$$\rho_B = mCTN_{low} + pCTN_{high} + q$$

Where [m, p, and q] are unknown coefficients that can be solved by setting up a system of equations with four 3 x 3 determinants. The CTN is obtained from the CT scans for each of the homogenous calibration standards.

In this study, the high and low energy image stacks were loaded into Python as arrays. A 3D Gaussian blur filter with a sigma of 2 was used to reduce noise in the images. The scipy.solv module of Python was then employed to solve for the coefficients based on the calibration CTN values. The ρ_B was solved for each pixel in the 3D volume and saved as two new separate image stacks.

3.4 COMPILED CORE LOG

The compiled core logs were scaled to fit on single pages for rapid review of the combined data from the medical CT scans and MSCL readings. Logs are presented for each of the cored sections from the Brush Creek Quarry Well, E. Miller/Hanna City Well, Morris Well, and Weatherford Well. All available cores were medically CT scanned. Each log includes the following tracks: track 1, U, Th, K (in percent); track 2, gamma density (black) and magnetic susceptibility (red); track 3, medical CT images (left light to show greyscale variations in coals; right, dark, to show variation in the rocks), cropped to center portion of images to highlight greyscale variations; track 4, elemental XRF mineralogy that are colored to indicate carbonates (blue, Mg + Ca), quartz (yellow, Si), clays (grey, Al; red, Fe; pink, K), and sulfuric minerals (gold, S); tracks 5, 6, 7, 8, and 9 proxy elemental measurements in parts per million; and track 10 shows a summation of rare earth elements (REE) elements that may lead as a proxy for enrichment in middle and heavy REEs outside of the resolution of the handheld XRF .

The elemental results from the XRF was used to display important elemental proxies related to detrital influence (Si, Al, K, Ti, and Zr in track 5), skeletal influx/carbonate potential (Ca, Mg, Mn, and Ba in track 6), redox potential (V, Cr, Co, Ni, Cu, and Mo in track 7), biogenic

production (V, P, Zn, and Y in track 8), and chalcophile (Pb, As, S, and Fe in track 9). Track 10 represents a summation of La, Ce, and Y that can be used to indicate enrichments in REEs.

The elemental proxy log also includes an XRF "mineralogy" with Al and K, representing clays; Ca, representing calcite; and Si, representing quartz, although there is some Si contribution to the clays. Pyrite (reduced) should have low magnetic susceptibility, and Fe oxide or hydroxide should have high magnetic susceptibility. These broad trends can quickly give information over large lengths of core and direct more focused research to zones of potential interest. These logs are presented in the following images (Figure 34 to Figure 37).

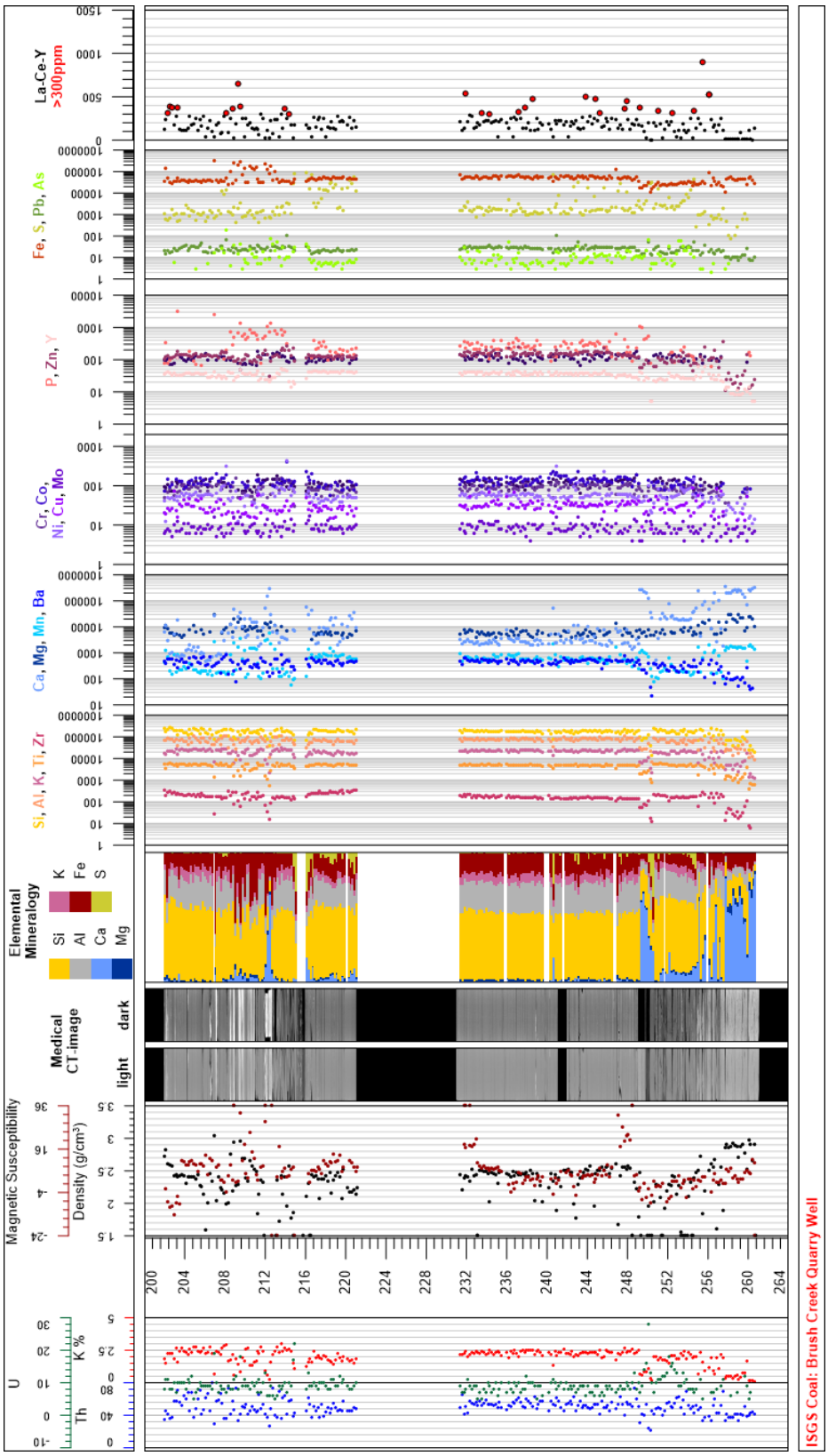

Figure 35: Compiled core log for the Brush Creek Well from 202–262 ft.

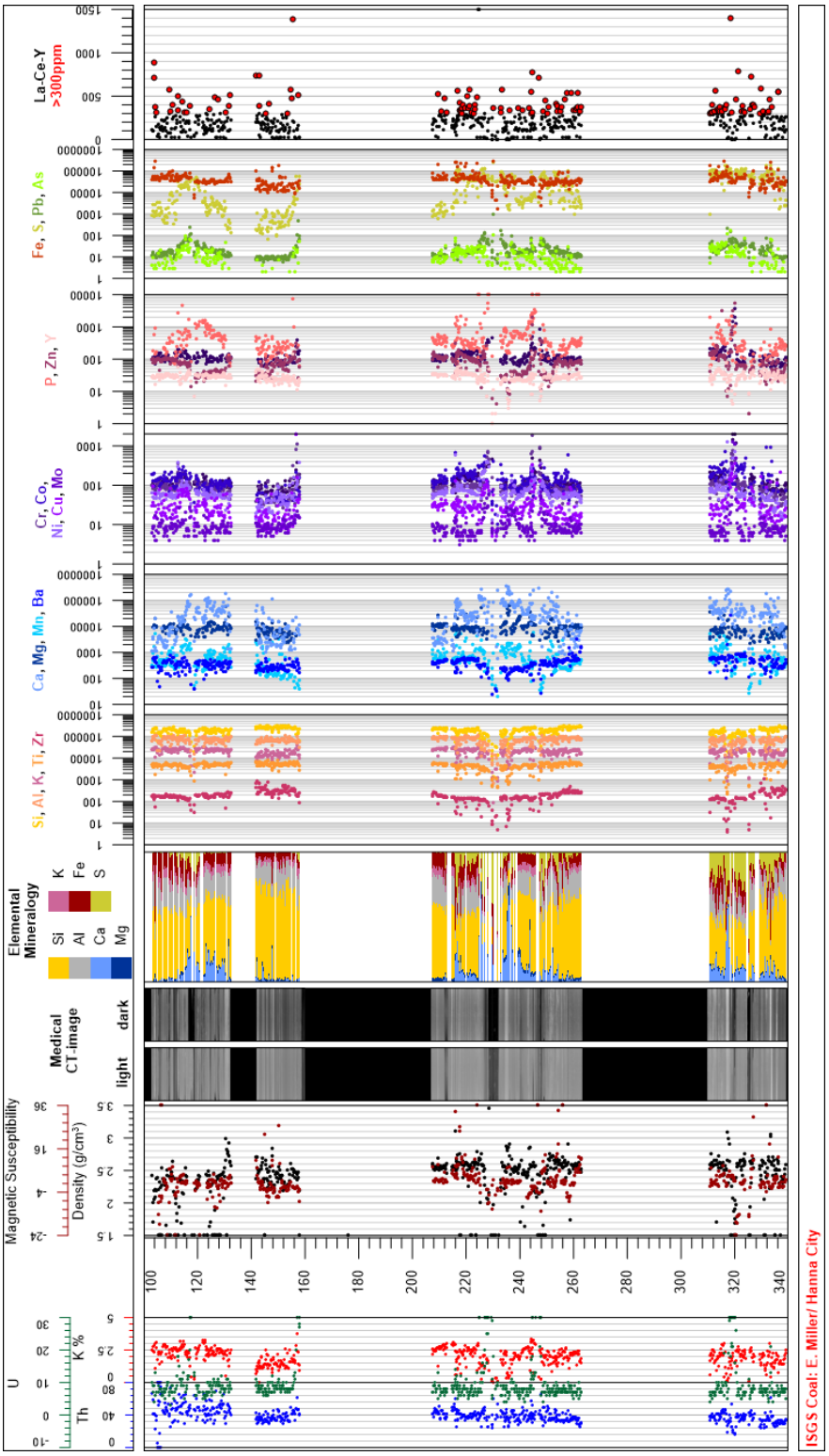

Figure 36: Compiled core log for E. Miller/Hanna City Well from 150–340 ft.

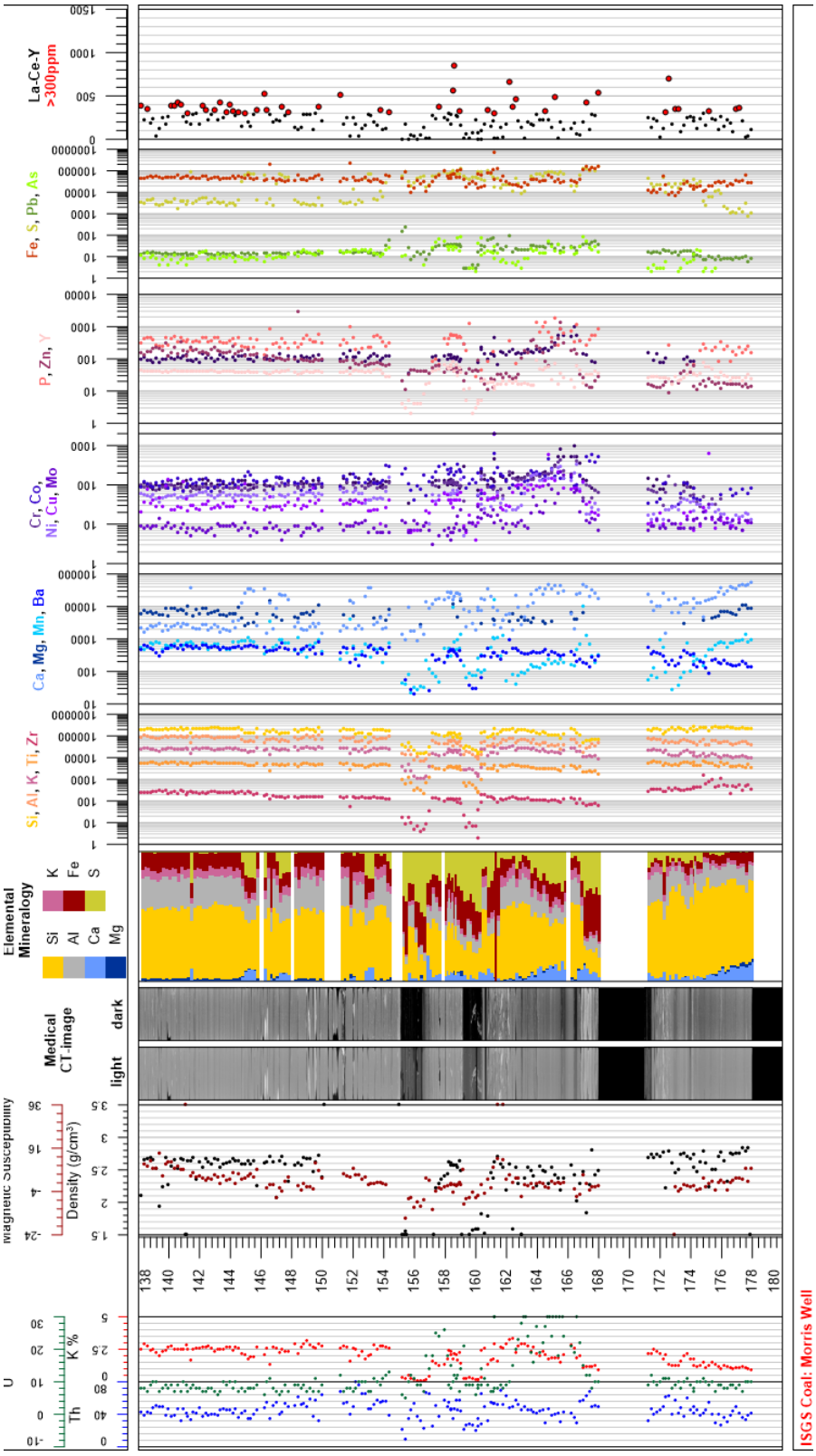

Figure 37: Compiled core log for Morris Well from 138–178 ft.

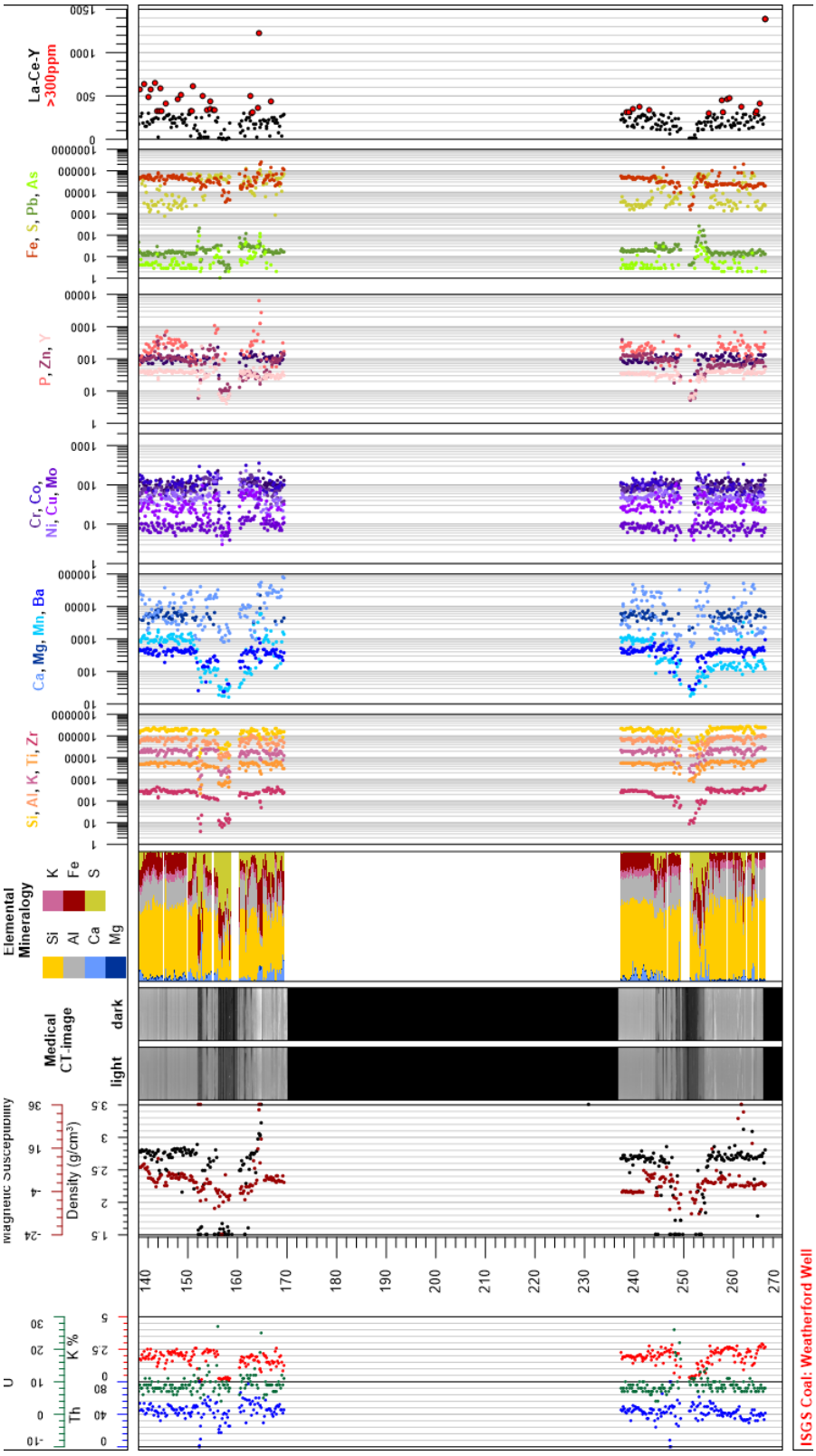

Figure 38: Compiled core log for Weatherford Well from 140–275 ft.

4. DISCUSSION

The evaluation of the magnetic susceptibility, elemental XRF, and CT analysis offers a unique look into the internal structure of the core and macroscopic changes in lithology. These methods:

- Are non-destructive
- When employed together, they offer a more thorough understanding of the core than any single technique alone
- Can be used to identify zones of interest for further detailed analysis, experimentation, and quantification
- Provide a detailed digital record of the core, before any destructive testing or further degradation, that is accessible and can be referenced for future studies.

5. REFERENCES

Denny, F. B. *Weatherford Stratigraphic Column*. Champaign, IL, 2005. https://isgs-oas.isgs.illinois.edu/reports/rwservlet?oilsummary&121452892900 (accessed December 2023).

Geotek Ltd. Multi-Sensor Core Logger Manual; Version 05-10; Published by Geotek, 3 Faraday Close, Daventry, Northamptonshire NN11 8RD, 2010. info@geotek.co.uk, www.geotek.co.uk

Hunts, C.; Moskowitz, B.; Banerjee, S. *Magnetic Properties of Rocks and Minerals;* Rock Physics and Phase Relations: A Handbook of Physical Constants; 1995; pp 189–204.

Iowa State University Center for Nondestructive Evaluation, Ames, IA, 2021. https://www.nde-ed.org/Physics/X-Ray/attenuation.xhtml (accessed July 2021).

Johnson, T. R. C. Dual-Energy CT: General Principles. *American Journal of Roentgenology* **2012,** *199*, S3–S8. DOI: 10.2214/AJR.12.9116.

Nelson, J. *Morris Stratigraphic Column,* Champaign, IL, 2004. https://isgs-oas.isgs.illinois.edu/reports/rwservlet?oilsummary&121992399600 (accessed December 2023).

Nelson, J.; Elrick S. *Brush Creek Quarry Stratigraphic Column.* Champaign, IL, 2010. https://isgs-oas.isgs.illinois.edu/reports/rwservlet?oilsummary&121732432400 (accessed December 2023).

Nelson, J.; Elrick S. *Miller Eric/Hanna City Stratigraphic Column.* Champaign, IL, 2012. https://isgs-oas.isgs.illinois.edu/reports/rwservlet?oilsummary&121433549100 (accessed December 2023).

Schneider, C. A.; Rasband, W. S.; Eliceiri, K. W. NIH Image to ImageJ: 25 years of image analysis. *Nature Methods* **2012,** *9*, 671–675.

Siddiqui, S.; Khamees, A. A. Dual-Energy CT-Scanning Applications in Rock Characterization. *Society of Petroleum Engineers* **2004**. DOI:10.2118/90520-MS.

This page intentionally left blank.

Marianne Walck
Director
National Energy Technology Laboratory
U.S. Department of Energy

Jessica Mullen
Critical Minerals Sustainability
Technology Director
National Energy Technology Laboratory
U.S. Department of Energy

Scott Montross
Critical Minerals Sustainability
Technology Director
National Energy Technology Laboratory
U.S. Department of Energy

Anna Wendt
DOE HQ Program Manager
Office of Resource Characterization
U.S. Department of Energy

Bryan Morreale
Associate Laboratory Director of the
Research and Innovation Center
National Energy Technology Laboratory
U.S. Department of Energy